EXPONENTIAL POTENTIALS IN KANTOWSKI-SACHS EINSTEIN-AETHER SCALAR FIELD COSMOLOGICAL MODELS

by

Sean A. O'Neil

Submitted in partial fulfillment of the requirements
for the degree of Master of Science

at

Dalhousie University
Halifax, Nova Scotia
September 2020

Table of Contents

List of Tables

List of Figures

Abstract

A class of positive curvature spatially homogeneous but anisotropic cosmological models within an Einstein-aether gravitational framework is investigated. The matter source is assumed to be a scalar field which is coupled to the expansion of the aether field through a generalized (constant plus exponential) potential $V = \Lambda + e^{-2k\phi} + a_2\theta e^{-k\phi}$. The evolution equations are expressed in terms of expansion normalized variables to produce an autonomous system of ordinary differential equations suitable for a numerical and qualitative analysis. An analysis of the local stability of the equilibrium points leads to the discovery of periodic orbits and we investigate the stability of these solutions as we generalize our model. We will analyze various sets of models in an attempt to investigate some of the underlying features of these models.

Acknowledgements

I would like to thank Dr. A.A. Coley, my supervisor. I would also like to thank Dr. Robert van den Hoogen, the first author of [1809.01458], which was published before this thesis was completed.

Chapter 1

Introduction

In 1930 Edwin Hubble discovered that light from distant objects was redshifted and observed that the further these objects were from us, the more they were redshifted [24]. When we refer to the cosmological redshift of light, we are referring to a feature of the underlying spacetime rather than just the relative motion of bodies as in the acoustic Doppler effect where one could imagine the change in pitch of sound coming from a siren travelling at an observer and then proceeding past. In other words, the light that Hubble observed must have been redshifted as a result of the space itself expanding. This was a huge discovery since it was long thought that the universe was static. Since Copernicus we have suspected that the Earth is not the 'center of the universe', and so if the observed light is redshifted more and more with distance and we are not the center of the expansion, then it can be concluded that all points in the universe are moving away from one another.

In the 1970's and 80's, the theory of inflation was developed by a number of prominent theoretical physicists (Linde, Guth et al.) [13]. Cosmological inflation is the idea that there was an acceleration of the expanse of space itself moments after the theorized big bang. It is hypothesized that inflation took place from somewhere on the order of 10^{-36}sec to $10^{-33} - 10^{-32}$sec. Shortly after the big bang the universe can be described as an opaque plasma because in this state, the density and temperature were so high that even photons were not freely moving in this plasma and so its impossible for us to 'see' anything before this state/point in time. Cosmic inflation was the mechanism by which the universe expanded rapidly and then cooled enough to allow for the beginning of the next epoch: recombination. Once the universe expanded enough, this opaque plasma cooled enough to form neutral atoms and these newly formed atoms, mostly hydrogen and helium with trace amounts of

lithium and other light elements, were allowed to settle to their ground state, emitting photons as a result. These photons are what we have mapped as the Cosmic Microwave Background (CMB-radiation, sometimes CMBR) with the Wilkinson Microwave Anisotropy Probe (WMAP)[26]. Again, this is the earliest radiation that we have been able to detect and this is not due to the physical limitations of our equipment, but rather because there is no radiation in the normal sense for us to detect before this time. The accepted theory is that before the universe undergoes inflation, the opaque plasma had tiny, quantum fluctuations in its density and when inflation occurred, these fluctuations grew to allow the matter densities to coalesce and form the large-scale structures - galaxies, clusters, voids, etc - that we can observe today. In other words, we can observe certain features of our universe today such as these galactic structures so whatever model we investigate, it necessarily has to present solutions in which these features are possible in order to match up with our present day observations.

A very important question is the one of 'same-ness' observed all around us through our telescopes. Any theory that we derive would have to explain why our observable universe appears to be uniform on large enough scales. This is nicely summarized into one idea. The Cosmological Principle states that the universe is spatially homogeneous and isotropic, meaning firstly that the same observational evidence is available to observers at different locations and, secondly, that the universe is the same in all directions [18]. These are two very closely related but separate ideas. A good way to consider the difference between the two is in the context of a magnetic field. A magnetic field is homogeneous since it fills a space and is the same at every point but it is not isotropic because it has a direction. If a model of the universe is isotropic in two or more spatial locations at a given point in time, then it is necessarily spatially homogeneous. Clearly the universe is not homogeneous on, say, the scale of our solar system since we observe voids between celestial bodies and other matter such as the asteroid belt, planets, moons, etc. Even on a galactic scale the Milky Way is not homogeneous since we can note its two main spiral arms and the relative voids which separate those structures. There is also clear structure that we can discern at nearby galaxies as well which clearly demonstrates non-homogeneity at certain scales. In

summary, any cosmological model we choose to study must answer questions about the spatial homogeniety and isotropy of the universe.

There are a few reasons why inflation is an attractive theory, but mainly it addresses the following three points which make the universe that we see around us today much more statistically likely than without this mechanism. These are collectively referred to as the cosmological fine-tuning of our universe - everything that exists in our universe today, including us, is due at least in part to the values of several fundamental constants (speed of light, Boltzmann constant, elementary charge, etc). If any of these values are tweaked by any amount then all of the fundamental interactions that people have studied would not occur as we know them and we could not exist. Inflation gives us a dynamical way in which our universe can evolve towards its current state.

The first reason is called the 'horizon problem'. This problem relates to the Cosmological Principle. Why is it that when we look at the temperature distribution in the CMB data, that the maximum differences are on the order of 10^{-5}K [26]? If the universe is very much the same wherever you look at this cosmic time, then it must have been even more uniform in the early universe. It appears that matter and energy would have come to an equilibrium in their distribution before inflation, and then once inflation took place, it propelled local energies very far away from one another. So when we look in the sky today and can observe the homogeneity and isotropy of the universe, distant regions of space (researchers think that one degree of angular seaparation in our sky is the limit for regions of space being causally connected in the early universe) could have theoretically interacted with each other before the period of inflation.

The second reason for the attractiveness of inflation is the flatness problem. This is similar to the Horizon problem but has to do with the spatial curvature of the universe. Essentially, we have measured the universe and the best estimate is that it is nearly flat ($\Omega = \Omega_{mass} + \Omega_{relativistic} + \Omega_{\Lambda} \approx 0.27 + 0.0000824 + 0.73 \approx 1.00 \pm 0.02$) [19] [6]. Even though we know the Earth to be round, on small enough scales it can

appear to be locally flat. Cosmological inflation tells us that although the universe may have had curvature at one point, the massive expansion of the universe means that to the highest level of precision we have, we appear to exist in a flat universe on large scales at the current time.

The last problem that inflation helps explain is that of the magnetic monopole problem. In fact, this was the main problem that Guth was trying to tackle in 1979 when he came up with the idea of cosmological inflation [13]. The basic concept is that a very hot, dense universe would have produced heavy magnetic monopoles that would still exist in the current era. All searches for these monopoles have failed. Inflation solves this problem by being initiated at a time after the monopoles have formed and thus their prevalence would be reduced by several orders of magnitude.

Now we want to discuss another aspect of this thesis; the aether. The 'Luminiferous Aether', as was originally referred to, was thought to be a medium in which the universe existed. At the time when this theory of the Luminiferous Aether was common, it was very popular for scientists to be investigating the properties of light and it had been known for some time that light could demonstrate both particle-like and wave-like properties [23] [7]. Water waves travelled through water, sounds waves through air and it was thought that light needed the Luminiferous Aether in order to propagate [7]. The aether can also be thought of in relation to Maxwell's electromagnetism in the late 1800's, as his equations unified the previously separate ideas of electricity and magnetism and predicted waves (of light) travelling at the speed of light and, at the time, this confounded scientists because in their view waves must have a medium in which to propagate [16]. In the following decades, various properties were continually attributed to the aether until it became ever more unlikely for it to actually exist. For example, since scientists at the time knew a great deal about how light interacted with other particles (e.g. the photoelectric effect) they hypothesized that the aether was an infinite material that existed everywhere in the universe that could not have interacted with any physical objects. There were many experiements that attempted to study how the aether might interact with the world around us but arguably the most famous is the Michelson Morely experiment

(1902-1905) [15]. Essentially, the scientists hypothesized that if the aether existed and that we on Earth were moving through the aether (remember that the aether itself was thought to be stationary) then they could try to measure the speed of light in two different directions and should have been able to detect slight differences in the speed of light since it would be interacting with the aether as the light waves propagated during the experiment. The experiment very famously produced a null result; that there was no detectable difference in the speed of light, regardless of the direction in which it was measured. These sorts of experiements were continued and the results repeated time and again. Even more recently, scientists have performed an experiment using lasers and it has further confirmed the absence of the aether to an order of 10^{-17} [14]. Eventually, the aether theory was all but discarded and instead the scientific community preferred Einstein's Special Relativity and subsequently his General Theory of Relativity.

So the important question is where does that leave our theory today? The aether field fell out of popularity when Einstein introduced his special and general theories of relativity which explained much of the same material without as many of the pitfalls [10]. Lately, the theory of the aether has been revisited for a few reasons. In 1998 Perlmutter, Schmidt and Riess used their observations of distant supernovae to determine that the universe was expanding at an accelerating rate and, in fact, won the Nobel prize for this discovery [11]. So how did scientists attempt to explain this? One simple answer is the aether. To be fair, this aether is not exactly the same as the Luminiferous Aether which we discussed earlier. However, this aether is still thought of as a 'vacuum energy' that persists throughout space and will drive the accelerated expansion of the universe [29]. Even during Einstein's time, he and his peers did not consider Special Relativity to completely remove the possiblility of an aether. In fact, many different explanations have existed since the 16th to 19th century but they would not be considered mathematically valid by modern standards.

Separate observations having to do with the celestial motion of galaxies has also yielded the hypothesis of so-called dark matter [5], whereas the invisible force that

is causing the accelerated expansion of the universe is referred to as dark energy. There is one more piece of this puzzle before we can get into the specifics about the models considered in this project and that is Einstein's cosmological constant. Einstein believed in a static (non-expanding) universe and so he originally included the cosmological constant to avoid the consequences of a purely dynamic universe. Later Einstein would famously refer to this addition to his equations as his 'biggest blunder'. We are now back at the beginning of our story when Hubble discovered the expanding universe in 1930 and Einstein realized he had failed to trust his equations which had predicted the same thing. Later on, the Nobel Laureates [22] [21] Perlmutter, Schmidt and Riess, discovered that the universe was not only expanding, but doing so at an accelerated rate, which brings us to the present where some scientists are adding the cosmological constant back into the equations (however, for different reasons than in the time of Einstein and Hubble).

As described in [29], General Relativity is a classical theory while matter fields are of a quanitzed nature. This observation leads to the conclusion that there must be a non-vanishing vacuum energy and we can write the stress-energy tensor for a perfect fluid in a vacuum state representing this vacuum energy as $T_{vac,\mu\nu} = -\rho_{vac} g_{ab}$, and this is true at every point in spacetime. The influence of this term and that of Einstein's so-called bare cosmological constant act in the same way and so they are combined into the 'effective cosmological constant' $\Lambda_{eff} \equiv \Lambda_{bare} + 8\pi G_N \rho_{vac}$. This allows us to write Einstein's equations succintly as:

$$G_{ab} + \Lambda_{_{eff}} g_{ab} = \frac{8\pi G_N}{c^4} T_{ab} \, , \tag{1.1}$$

The issue is that we can both estimate the accelerated expansion of the universe and the relative sizes of the quantities in the equation for Λ_{eff} with CMB data and standard candles and there turns out to be a massive difference between what the theory predicts and what we have observed [29]. One way to address this problem is the gravitational aether we have been talking about (that is also modeled as a fluid with a shear term here). This is classified as a matter-modifying theory since we can decouple the vacuum energy from the geometry and a term is moved to the matter side of the field equations.

Chapter 2

Background

Quantum gravity may predict a preferred rest frame at the microscopic level in vacuum necessitating a violation of Lorentz invariance. Further, in cosmology there is a natural frame associated with the cosmic microwave background, and therefore it is possible the assumption of Lorentz invariance may need to be relaxed even at the macroscopic level [9] [25] [26] [1]. This idea goes back to the original proposition of the 'Luminiferous Aether' that we discussed in the last section. Fortunately, a gravitational theory that violates Lorentz invariance while maintaining general covariance has been proposed within a relativistic framework, which could possibly address these concerns from both the micro and macroscopic perspectives.

Einstein-aether theory consists of an aether vector field that spontaneously breaks Lorentz invariance by selecting a preferred direction at each spacetime point while maintaining local rotational symmetry. It is only the boost sector of the Lorentz symmetry that is actually broken. In this effective field theory, the local space-time structure is determined by a dynamical time-like vector field, u^a (the aether), together with the metric tensor, g_{ab} [12].

In Einstein-aether theory with inflation caused by a scalar field there exists the possibility that the inflation is affected by the aether through a direct coupling of the scalar field with the aether field through the expansion and/or shear of the aether vector field. In particular, Donnelly and Jacobson found that the scalar field/aether field coupling can either slow down or speed up the evolution of inflation within a chaotic inflationary scenario [8].

We shall investigate a class of locally spherically symmetric and spatially homogeneous Einstein-aether cosmological models containing a scalar field using a $1 + 3$

formalism. It is assumed that the scalar field and aether field are coupled to each other through the scalar field potential (and physical parameters). In particular, we explore the possible impact of the scalar field/aether field coupling within these so-called Kantowski-Sachs scalar field models having a generalized constant plus exponential potential plus a coupling term betweeen the scalar field and aether field [27].

2.1 The Geometry

This section follows [2] and [27]. The action under consideration contains a Lagrangian for Einstein-aether (AE) gravity together with a Lagrangian for the matter field (M):

$$S = \int d^4x\sqrt{-g}\left(\frac{1}{8\pi G}L^{AE} + L^M\right) \tag{2.1}$$

The Lagrangian for AE and M are, respetively:

$$L^{AE} = \frac{1}{2}R - K^{ab}_{cd}\nabla_a u^c \nabla_b u^d + \lambda(u^a u_a + 1) \tag{2.2}$$

and

$$L^M = -\frac{1}{2}g^{ab}\nabla_a\phi\nabla_b\phi - V(\phi,\theta,\sigma^2) \tag{2.3}$$

where $K^{ab}_{cd} = c_1 g^{ab}g_{cd} + c_2\delta^a_c\delta^b_d + c_3\delta^a_d\delta^b_c + c^4 u^a u^b g_{cd}$, λ is the Lagrange multiplier, $\theta = \nabla_a u^a$ is the expansion scalar and $\sigma^2 = \frac{1}{2}\sigma_{ab}\sigma^{ab}$ is the shear scalar and u^a is the aether vector. V is the potential and the c_i are arbitrary coupling constants. The 'Kantowski-Sachs' part of this project comes from the metric that we will use. This metric is one that describes a spatially homogeneous but anisotropic universe. The spherically symmetric spatially homogeneous Kantowski-Sachs models under consideration have a four-dimensional group of isometries acting non-transitively on three dimensional spatial hyper-surfaces. Here we shall assume that the aether vector field is invariant under the same group of symmetries as the metric and is consequently aligned with the symmetry adapted time coordinate and is hyper-surface normal. In co-moving coordinates adapted to the symmetries of the metric we write $u^a = (1,0,0,0)$ and

express the Kantowski-Sachs Metric as:

$$ds^2 = -dt^2 + a(t)^2dx^2 + b(t)^2(dv^2 + sin^2(v)d\psi^2) \tag{2.4}$$

The general terms that appear in the models are introduced in [27] and [20] and these equations are for the specific case where the matter source is a scalar field. With the assumptions on the metric and aether vector, we have that the vorticity and acceleration of the aether vector are zero and we can calculate the covariant derivative $\nabla_b u_a$. This covariant derivative depends on the expansion scalar, shear tensor (and shear scalar). In particular, these terms are given below:

$$\begin{aligned}
\nabla_b u_a &= \sigma_{ab} + \frac{1}{3}\theta(g_{ab} + u_a u_b) \\
\theta &= \nabla_a u^a = \frac{\dot{a}}{a} + 2\frac{\dot{b}}{b} \\
\sigma_{ab} &= u_{a;b} - \frac{1}{3}\theta(g_{ab} + u_a u_b)
\end{aligned}$$

where $\sigma_a^b = Diag[0, -2\sigma_+, \sigma_+, \sigma_+]$ and $\sigma_+ = \frac{1}{3}\left(\frac{\dot{b}}{b} - \frac{\dot{a}}{a}\right)$ and the shear scalar is $\sigma^2 = 3\sigma_+^2$. Together with the definition of the energy momentum tensor for the aether field, we can now write the equations for the effective energy density, isotropic pressure, energy flux, and anisotropic stress, which will all depend on the parameters c_θ, c_σ which have been defined in terms of the c_i from above. We do this on page 11 after introducing the field equations.

In this thesis we are going to look at 3 different models. First, we will look at a single scalar field cosmology with an exponential and constant-plus-exponential potential. Second, we will look at a true Kantowski-Sachs model with an exponential potential. Finally, we will look at the same model as in Case II but modified to include a term in the potential that represents the cosmological constant. In general, we are going to reduce the Einstein-ather field equations, including the Raychaudhuri equation and the equation for the scalar field and potential, into a bounded system of ordinary differential equations and then study the evolutionary dynamics qualitatively from this perspective. We are going to analyze the equilibrium solutions and the behavior of the system in a neighborhood of these solutions to get a local picture

of the dynamics and then with an exhaustive list of equilibrium points and their local dynamical behaviour, we can make inferences about the behaviour of the system on a global scale. This method of study for these types of systems of equations, each of which is highly non-linear, is common since very often there are no exact solutions possible. This method allows us to greatly simplify things and find the equilibrium states of the resultant dynamical system, determine the local behaviour and then try to extrapolate and determine the global dynamics so that we can make some broad conclusions.

Varying the action (1.1) above with respect to the inverse metric g^{ab}, the aether vector u^a, the scalar field ϕ, and the Lagrange multiplier λ yields the Einstein-aether, Klein-Gordon and the normalization field equations (derived in [2]) which are:

$$G_{ab} = T^U_{ab} + 8\pi G T^M_{ab} \tag{2.5}$$

$$-2\lambda u_a = \frac{\delta L^U}{\delta u^a} + 8\pi G \frac{\delta L^M}{\delta u^a} \tag{2.6}$$

$$\nabla^a \nabla_a \phi - V_\phi = 0 \tag{2.7}$$

$$u^a u_a = -1 \tag{2.8}$$

Below we display the energy momentum tensors due to the aether field (U) and scalar field (M), respectively:

$$(aether field\, U) \qquad \begin{aligned} T^U_{ab} = {} & 2\nabla_c \left(J_{(a}{}^c u_{b)} - J^c{}_{(a} u_{b)} - J_{(ab)} u^c \right) \\ & + 2c_1 \left((\nabla_a u^c)(\nabla_b u_c) - (\nabla^c u_a)(\nabla_c u_b) \right) - 2c_4 \dot{u}_a \dot{u}_b \\ & - 2 \left(u^d \nabla_c J^c_d + c_4 \dot{u}_c \dot{u}^c \right) u_a u_b - g_{ab} \left(K^{cd}_{ef} \nabla_c u^e \nabla_d u^f \right) \end{aligned}$$

$$(scalar field\, M) \qquad \begin{aligned} T^M_{ab} = {} & \nabla_a \phi \nabla_b \phi - \left(\frac{1}{2} \nabla_c \phi \nabla^c \phi + V \right) g_{ab} \\ & + \theta V_\theta g_{ab} + \dot{V}_\theta h_{ab} \\ & + (\theta V_{\sigma^2} + \dot{V}_{\sigma^2}) \sigma_{ab} \end{aligned}$$

The Einstein-ather field equations are then:

$$0 = -\frac{1}{3}(1+c_\theta)\theta^2 + 3(1-2c_\sigma)\sigma_+^2 - {}^3R + 8\pi G\rho^M$$
$$0 = -(1+c_\theta)\dot{\theta} - \frac{1}{3}(1+c_\theta)\theta^2 - 6(1-2c_\sigma)\sigma_+^2 - \frac{8\pi G}{2}(\rho^M + 3p^M)$$
$$0 = (1+2c_\sigma)\dot{\sigma_+} + (1-2c_\sigma)\theta\sigma_+ + \frac{{}^3R}{3} - 8\pi G\pi_+^M$$

In terms of renormalized constant parameters c_σ and c_θ the different components of the Einstein-ather Field equations come from the energy momentum tensor due to the aether field (U). Note that the below equations do not represent a perfect fluid since perfect fluids do not have shear stresses, viscosity or heat conduction and we are including anisotropic stress to be in line with our assumption regarding out use of the Kantowski-Sachs metric. The different components are the effective energy density ρ^U, the isotropic pressure p^U, the energy flux q_a^U and anisotropic stress $\pi_b^{a\ U}$:

$$\rho^U = -\frac{1}{3}c_\theta\theta^2 - 6c_\sigma\sigma_+^2$$
$$p^U = \frac{1}{3}c_\theta\theta^2 + \frac{2}{3}c_\theta\dot{\theta} - 6c_\sigma\sigma_+^2$$
$$q_a^U = 0$$
$$\pi_b^{aU} = 2c_\sigma(\dot{\sigma}_b^a + \theta\sigma_b^a)$$

When we do some of the later calculations, we will redefine some of the above parameters for convenience. We will assume new units so that $\frac{8\pi G}{1+c_\theta} = 1$ and we will define $c^2 = C = \frac{1-2c_\sigma}{1+c_\theta}$, where $c = 1$ corresponds to general relativity. We can also define the curvature of the three-dimensional surfaces of homogeneity, which is given by ${}^3R = \frac{1}{b(t)^2} \geq 0$ for Kantowski-Sachs and ${}^3R = K$ for isotropic models where K can be positive, negative or zero. [27].

2.2 Scalar Fields With Exponential Potentials

The simplest model that yields an inflationary theory is that which has a single scalar field minimally coupled to gravity. This theory is generally consistent with the latest CMB data [1]. Quadratic and monomial potentials are in conflict with observations, predicting larger than expected tensor-to-scalar ratios. This makes models with a

simple exponential potential more attractive. The exponential potential of the form $V = e^{-2k\phi}$ naturally appears in higher dimensional fundamental theories and, from a mathematical perspective, the resulting system of dynamical equations has a scaling invariance that allows for the use of dimensionless variables [27]. However, these exponential potentials face their own issues [3]. They do, however, lead to a power law inflation if the potential is not too steep: $k^2 < \frac{1}{2}$. There have been other theories proposed that consider multiple scalar fields. In this case, we may actually achieve power-law inflation even if the individual parameters yield potentials that are too steep. This phenomenon is called assisted inflation [4]. We are going to look at $V = \epsilon\left(\Lambda + a_2\theta e^{-k\phi}\right) + e^{-2k\phi}$ where $\epsilon = 0, 1$ so we can consider the simple potential we mentioned above and a more complicated one when $\epsilon = 1$. We will consider these concurrently in the first case (with $a_2 = 0$ as there is no aether field coupling) since the algebra is relatively straightforward.

2.3 The Scalar Field Potential

The potential with constant and higher order correction terms is taken to be:

$$V(\phi, \theta, \sigma_+) = a_1 e^{-2k\phi} + a_2\theta e^{-k\phi} + a_3\sigma_+ e^{-k\phi} + \Lambda$$

Previous work [27] assumes that the parameters $k \geq 0$, $a_1 \geq 0$, but put no restrictions on the signs of a_2, a_3. For our particular analysis, we will set $a_1 = 1$, $a_3 = 0$ and make no assumptions about a_2. We will also only consider some particular invariant sets ($Q = 1, Q > 0$) in the dynamical system, but more on that later. Thus, our potential has the form:

$$V = e^{-2k\phi} + a_2\theta e^{-k\phi} + \Lambda \tag{2.9}$$

With this, we can write the equations for the effective energy density, isotropic pressure, energy flux and anisotropic stress due to the scalar field above which are all explicitly given in [27]. In particular, the Klein Gordon equation becomes:

$$0 = \ddot{\phi} + \theta\dot{\phi} - 2ke^{-2k\phi} - a_2 k\theta e^{-k\phi} \tag{2.10}$$

Chapter 3

Analysis

3.1 Case I - No Shear, (Constant-Plus) Exponential Potential ($a_2 = 0$)

We return to the case with no shear and both a purely exponential and constant-plus-exponential potential at the same time since the algebra is fairly straightforward. This is also meant to help illustrate the techniques we are going to use for the other two cases which are more complex. The Raychaudhuri equation and equations for the scalar field and potential are as follows:

$$\dot{D} = -\frac{1}{2}\dot{\phi}^2 - D^2 + \frac{1}{3}\left(\frac{1}{2}\dot{\phi}^2 + V\right) \tag{3.1}$$

$$V = V_0\left(\epsilon + e^{-2k\phi}\right) \tag{3.2}$$

$$\ddot{\phi} + 3D\dot{\phi} + V' = 0 \tag{3.3}$$

where $\epsilon = 0, 1$ depending which potential we are using and the Hubble parameter $D = \sqrt{\frac{1}{3}\left(\frac{1}{2}\dot{\phi}^2 + V\right) + K}$ where $K = -(\dot{D} + \frac{1}{2}\dot{\phi}^2)$. K is the dimensionless-normalized version of $k = -1, 0, 1$ from the FLRW metric, representing negative, zero and positive spatial curvature, respectively. It is derived from the first Einstein-aether field equation from page 10. Again this is only a simple single scalar field cosmology and is not a true Kantowski Sachs model. We would like to have a system with bounded variables so we are going to manipulate (3.1) above:

$$\begin{aligned} 1 &= \frac{\dot{\phi}^2}{6D^2} + \frac{V}{3D^2} + \frac{K}{D^2} \\ \Rightarrow 1 - \frac{K}{D^2} &= \frac{\dot{\phi}^2}{6D^2} + \frac{V_0\epsilon}{3D^2} + \frac{V_0 e^{-2k\phi}}{3D^2} \end{aligned}$$

In the above line, the terms on the right are bounded as long as we consider the $k = 0, -1$ cases. If we were to choose $k = 1$ than our analysis would no longer be from the context of bounded, compact phase space. For the below analysis, we

restrict our attention to the negative and zero spatial curvature situations. We choose the dimensionless normalized variables below. Note that $\epsilon = 1$ for the full 3×3 case shown.

$$\Psi^2 = \frac{\dot{\phi}^2}{6D^2} \qquad x^2 = \frac{V_0}{3D^2} \qquad \Phi^2 = \frac{V_0 e^{-2k\phi}}{3D^2} \qquad \frac{d}{dt} = \frac{1}{D}\frac{d}{d\tau}$$

Now we can differentiate the above to get new normalized equations. We will show the calculation for one of the variables, Ψ, to demonstrate the process. Keep in mind that derivatives are now taken with respect to the new time variable τ defined above (so when we differentiate below there is an extra factor of $\frac{1}{D}$ that appears). Then we can just use equations (3.1, 3.2, 3.3) to substitute into the result until we get something that is entirely in terms of the new variables:

$$\begin{aligned}
\Psi' &= \frac{1}{D}\left(\frac{\sqrt{6}D\ddot{\phi} - \sqrt{6}\dot{D}\dot{\phi}}{6D^2}\right) \\
&= \frac{-3D\dot{\phi} - V'}{\sqrt{6}D^2} - \frac{\sqrt{6}\left(\frac{-1}{2}\dot{\phi}^2 - K\right)\left(\sqrt{6}\Psi D\right)}{6D^3} \\
&= -3\Psi + \frac{-2kV_o e^{-2k\phi}}{\sqrt{6}D^2} + \frac{6\Psi^3 D^3 \frac{1}{2}}{D^3} + \frac{KxD}{D^3} \\
&= -3\Psi - 2k\frac{V_o e^{-2k\phi}}{\sqrt{6}D^2} + 3\Psi^3 + \Psi(1 - \Psi^2 - x^2 - \Phi^2) \\
&= \Psi(-2 + 2\Psi^2 - x^2 - \Phi^2) - \sqrt{6}k\Phi^2
\end{aligned}$$

Succinctly, we can write the equations as follows:

$$\Psi' = \Psi(q - 2) - \sqrt{6}k\Phi^2 \tag{3.4}$$

$$x' = x(q + 1) \tag{3.5}$$

$$\Phi' = \Phi(q + 1 + \sqrt{6}k\Psi) \tag{3.6}$$

where

$$\frac{-K}{D^2} = -1 + \Psi^2 + x^2 + \Phi^2 \tag{3.7}$$

$$q = 2\Psi^2 - x^2 - \Phi^2 \tag{3.8}$$

This full 3D system accounts for the cosmological constant term but if we just wanted to consider the case with the purely exponential potential then we can set $x = 0$ in all of the above, resulting in a 2D system. Now we can solve for all the

ID	Coords. $\{\Psi, x, \Phi\}$	Decel.(q)	Curv	Eigenvalues
a	0, 0, 0	0	-1	-2, 1, 1
b	1, 0, 0	2	0	3, 4, $3+\sqrt{6}k$
c	-1, 0, 0	2	0	3, 4, $3-\sqrt{6}k$
d	0, 1, 0	-1	0	0, -2, -2
e	$-\frac{\sqrt{6}k}{3}, 0, \frac{1}{3}\sqrt{9-6k^2}$	$2k^2-1$	0	$2k^2, 2k^2-3, 4k^2-2$
f	$-\frac{1}{\sqrt{6}k}, 0, \frac{1}{\sqrt{3}k}$	0	$\frac{1}{2k^2}-1$	$1, -1\pm\sqrt{\frac{2}{k^2}-3}$

Table 3.1: Equilibria for Case Ia and Ib

equilibrium points of the above by setting the LHS of the equations to zero and finding all the variables combinations where the equations are satisfied. In order to determine the stability of all these points we can linearize, use the Jacobian matrix and determine the eigenvalues at each of the equilibrium points. The Jacobian matrix for the full 3x3 system is:

$$\begin{pmatrix} 6\Psi^2 - x^2 - \Phi^2 - 2 & -2\Psi x & -2\Psi\Phi - 2\sqrt{6}k\Phi \\ 4\Psi x & 2\Psi^2 - 3x^2 - \Phi^2 + 1 & -2x\Phi \\ 4\Psi\Phi & -2x\Phi & 3\sqrt{6}k\Phi^2 + 2\Psi^2 - x^2 - 3\Phi^2 + 1 \end{pmatrix}$$

and for the 2x2 subsystem ($x = 0$) we would have:

$$\begin{pmatrix} 6\Psi^2 - \Phi^2 - 2 & -2\Psi\Phi - 2\sqrt{6}k\Phi \\ 4\Psi\Phi & 3\sqrt{6}k\Phi^2 + 2\Psi^2 - 3\Phi^2 + 1 \end{pmatrix}$$

We can neatly summarize all of the equilibrium points, the stability of those points, and the deceleration parameter, in one table that follows (and note again that the reduced 2x2 system is a subset of the full 3x3 system so the table below is an exhaustive list):

As we can see from the table above, there is a zero eigenvalue for point d), and so we can't immediately make any conclusions about the stability of these points. In order to analyze this, we use the center manifold theorem. In order to do this, we first must rescale our system so that the point d) is at the origin. We make the substitution: $x_{new} = x - 1$ and get the following system:

$$\Psi' = -\Phi^2\Psi + 2\Psi^3 - \Psi x^2 + 2\Psi x - 3\Psi - \sqrt{6}k\Phi^2 \tag{3.9}$$

$$x' = -\Phi^2 x + 2\Psi^2 x - x^3 + \Phi^2 - 2\Psi^2 + 3x^2 - 2x \tag{3.10}$$

$$\Phi' = -\Phi^3 + 2\Phi\Psi^2 - \Phi x^2 + 2\Phi x + \sqrt{6}k\Phi\Psi \tag{3.11}$$

Now, we first let Ψ and x be functions of Φ where we can discard the constant and linear terms since we already have the results from the linearization:

$$h = \begin{pmatrix} \alpha_1\Phi^2 + ... \\ b_1\Phi^2 + ... \end{pmatrix}$$

Following the steps outlined in the book by Wiggins [28], we set each of the following:

$$A = 0, \qquad f(\Psi, x, \Phi) = -\Phi^3 + 2\Phi\Psi^2 - \Phi x^2 - 2\Phi x + \sqrt{6}k\Phi\Psi$$
$$B = \begin{pmatrix} -3 & 0 \\ 0 & -2 \end{pmatrix} \qquad g(\Psi, x, \Phi) = \begin{pmatrix} -\Phi^2\Psi + 2\Psi^3 - \Psi x^2 - 2\Psi x - \sqrt{6}k\Phi^2 \\ -\Phi^2 x + 2\Psi^2 x - x^3 - \Phi^2 - 2\Psi^2 + 3x^2 \end{pmatrix}$$

We need to solve the following PDE in order to deduce the dynamics of the system near the equilibrium point. We can plug in everything we have defined above and solve to get a vector-valued equation and solve for the coefficients as follows:

$$\begin{aligned} N(h(x)) =& Dh(x)\left(Ax + f(h(z), z)\right) - Bh(z) - g = 0 \\ \Rightarrow & \begin{pmatrix} \sqrt{6}k\Phi^2 + 3\alpha_1\Phi^2 - 2\alpha_1 b_1\Phi^4 + ... \\ \Phi^2 + 2b_1\Phi^2 + b_1\Phi^4 + ... \end{pmatrix} = 0 \end{aligned}$$

Now we can solve for α_1 and b_1 so that the last statement above is true. These give us expressions for Ψ and x in terms of Φ (which we only had to take to order Φ^2):

$$\Psi = -\frac{\sqrt{6}k}{3}\Phi^2 + \mathcal{O}(\Phi^4)$$
$$x = -\frac{1}{2}\Phi^2 + \mathcal{O}(\Phi^4)$$

Following [28], we substitute these into equation (3.11) and, the dynamics of the center manifold near the equilibrium point will be completely governed by the equation:

$$\begin{aligned}\Phi' &= -\Phi^3 + 2\Phi\Psi^2 - \Phi x^2 - 2\Phi x + \sqrt{6}k\Phi\Psi \\ &= -2k^2\Phi^3 + \mathcal{O}(\Phi^4)\end{aligned}$$

Since Φ is greater than zero (because $V_0 > 0$ and $e^{k\phi} > 0$), the function $\Phi' = -2k^2\Phi^3$ is always negative to the right of zero and so Φ' is always negative. Therefore, the orbits are future stable on the center manifold and so the point for which $(\Psi, x, \Phi) = (0, 1, 0)$ is stable.

There are a few main ranges of the parameter k for which the qualitative behavior is different. These are $k < \sqrt{2/3}$, $\sqrt{2/3} < k < \sqrt{3/2}$, $k > \sqrt{3/2}$. To make a few quick conclusions about the system in general, we can see that point b) is a source for all parameter values, point d) is a sink for all parameter values, and the rest are either saddles with varying numbers of stable and unstable manifolds, or sources depending on the parameter values. Points a) and f) are the only points with non-zero curvature and point f) has a value for which the curvature changes from positive to negative at $k = \sqrt{1/2}$. Point d) is inflationary for all parameter values and point e) switches from inflationary to non-inflationary at $k = \sqrt{1/2}$. The full details of the stability of all the equilibrium points can be summarized in the table below. The 's' and 'us' refer to the number of stable and unstable manifolds for the saddle point. For instance, '2D-s, 1D-us' would refer to a saddle point which has a two-dimensional stable manifold and one-dimensional unstable manifold:

ID	$k < \sqrt{2/3}$	$\sqrt{2/3} < k < \sqrt{3/2}$	$k > \sqrt{3/2}$
a	1D-s, 2D-us	1D-s, 2D-us	1D-s, 2D-us
b	source	source	source
c	source	source	1D-s, 2D-us
d	sink	sink	sink
e	saddle (stability switch at $\sqrt{1/2}$)	1D-s, 2D-us	source
f	1D-s, 2D-us	2D-s, 1D-us	2D-s, 1D-us

Table 3.2: Stability for Case Ia and Ib

Recall that since we redefined the variable according to $\frac{d}{dt} = \frac{1}{D}\frac{d}{d\tau}$, that $\tau \to -\infty$ is equivalent to $t \to 0^+$. Based on this we can see that the sources (early time attractors) are solutions where the scalar field is present. The sink (late time attractor) is the solution that only contains the constant factor of the potential, and so the scalar field is dynamically negligible at late times. The late time behavior of the system is also inflationary for all parameter values and the curvature tends to zero. Thus we have a system such that for all values of the parameter, the solutions tend to a solution which does not depend on the scalar field, is inflationary and has zero curvature. Thus we have another example of a dynamical model that can realize inflation. We can also note that there is a solution (saddle/source depending on the parameter value) that is inflationary for some parameter values ($k < \sqrt{1/2}$) and so the behavior of the system could evolve toward a state where the scalar fields make up a significant part of the energy density and remain close to this state for arbitrarily long periods of time.

This model can be thought of as a purely exponential potential evolving in a ΛCDM background, which can be seen from the choice of normalized variables. This tells us that the constant term in the potential has the same influence as a cosmological constant. For this model, the scalar fields evolve first like matter, and then like a cosmological constant, but it is not the same as simply adding a dark matter term at early times and a cosmological constant at late times (it is dynamical so there is a slow decay to a constant at late times). Also, if k is found to be large enough, then this model is nearly indistinguishable qualitatively from the ΛCDM model.

This model predicts that inflation will occur for any value of k and once the solution begins to inflate, it won't stop. The article [3] also suggests that $k > 13$ based on recent supernova data. The other issue with this model is that it only partially solves the coincidence problem. V_0 must be constant to match with the current dark energy density which left us with only k as a free parameter. The model has to be tuned so that the constant term begins to dominate the pure exponential term as is what we think is happening in the current era.

This analysis can be supported with some numerics. For the plots below, the numerics have been carried out in python and have been solved using the Runge-Kutta (Dormand-Prince, 4/5th order) method for solving autonomous ODE's. The solutions that are colored red indicate the forward time evolution solutions and the blue represent the backward solutions. For the 3D plots, the view from the $(+,-,+)$ and $(+,+,-)$ octants are shown for each parameter case. The first three plots are regarding the first subcase of the above system which is just a 2x2 system. The first plot shows the numerics with a parameter value of $k = 0.8$, the second with $k = 1.1$ and the third with $k = 1.5$ - so that the three cases cover the parameter ranges for which the most significant qualitative dynamics occur for the system. We can also show some numerics for the full 3x3 system. We will use similar parameter values as in the previous examples for easy comparison. In fact, in some of these plots it is interesting to see that the limiting orbit (a (half) circle, derived from the first integral) from the last case is still clearly visible in these plots. The circle is skewed due to the scale in the below images and so it looks like an ellipse rather than a circle. We also only show the upper half plane since $\Phi > 0$ and so the lower half plane is meaningless. In the first set of plots, Ψ is on the x-axis and Φ is on the y-axis. When we add the new variable in the second set of plots, Ψ remains on the x-axis, Φ is on the z-axis and x is on the y-axis.

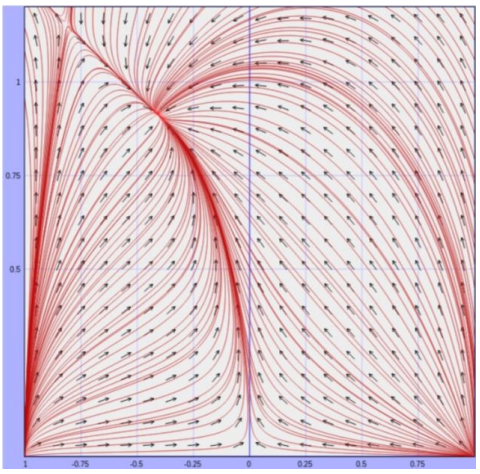

Figure 3.1: Case Ia (2x2) - k=0.5

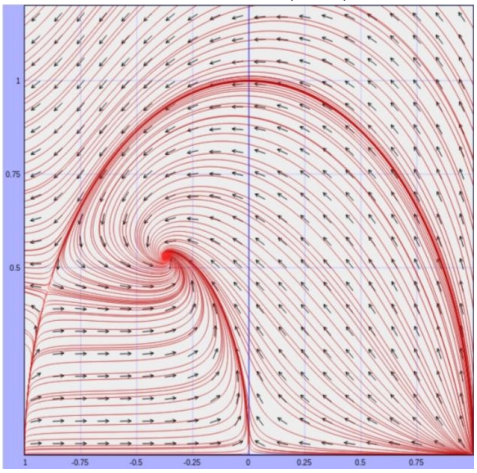

Figure 3.2: Case Ia (2x2) - k=1.1

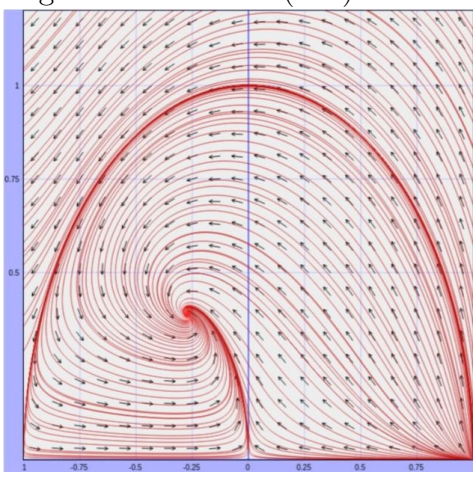

Figure 3.3: Case Ia (2x2) - k=1.5

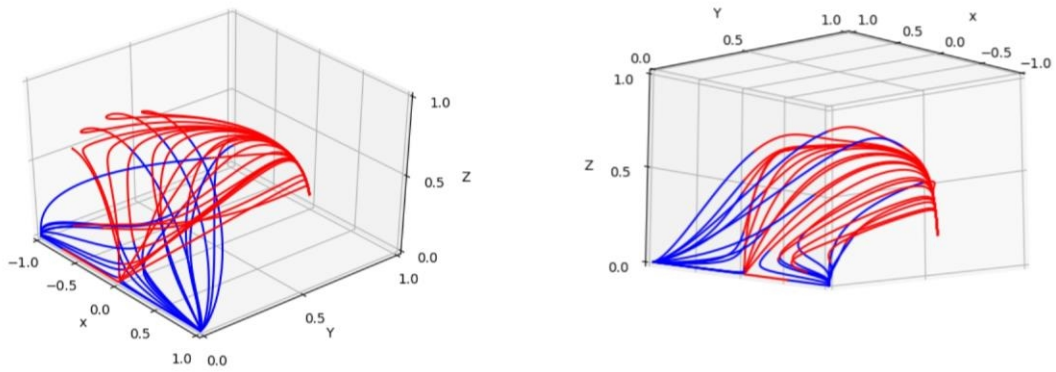

Figure 3.4: Case Ib (3x3) - k=0.8

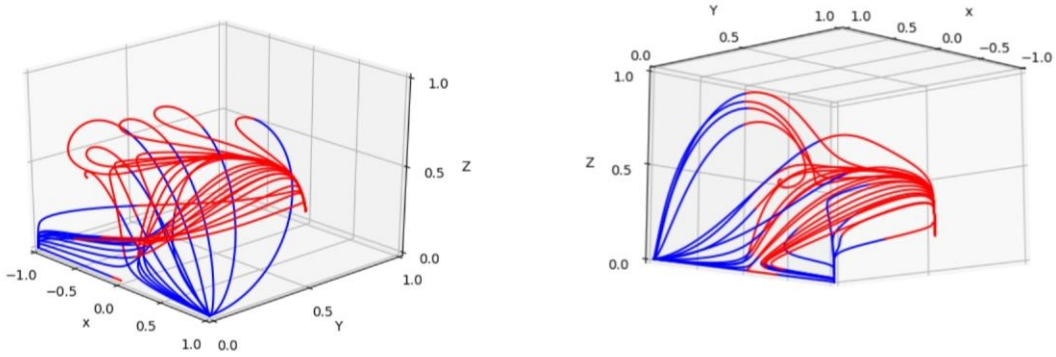

Figure 3.5: Case Ib (3x3) - k=1.1

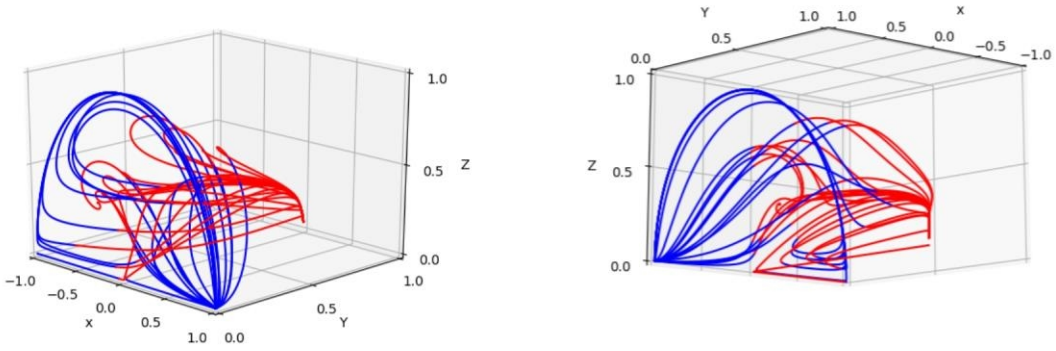

Figure 3.6: Case Ib (3x3) - k=1.5

3.2 Case II - Shear, Exponential Potential

In this case we are going to include the shear term, the scalar-aether field coupling term ($a_2 \neq 0$) and an exponential potential. This is a true Kantowski-Sachs model, utilizing the KS metric. What is interesting about this particular model, as was studied in [27], is that in one of the invariant sets we can find an infinite set of periodic orbits (for a specific set of bounds on the parameters). This sort of behaviour is particularly interesting, which is why we will investigate it further in Case III and why we need further analysis than in the previous section. Specifically, in the final section we will see if using the constant plus exponential potential instead of just the exponential potential will destroy the periodic orbits or if they will persist as an underlying feature of the model.

Variables Φ and Ψ have similar definitions as in Case I. We define $D = \sqrt{\frac{1}{1+c_\theta}\frac{1}{b^2} + \frac{1}{3}\theta^2}$. The variable defintions are:

$$\Psi = \frac{\dot{\phi}}{\sqrt{2}D} \qquad \Phi = \frac{e^{-k\phi}}{D} \qquad y = \frac{\sqrt{3}\sigma_+}{D} \qquad Q = \frac{\theta}{\sqrt{3}D} \qquad \frac{d}{dt} = \frac{1}{D}\frac{d}{d\tau}$$

The dimension normalized variables and equations following Case I, and derived in [27], are:

$$\frac{d\Phi}{d\tau} = -\Phi\left(\sqrt{2}k\Psi + \chi\right) \tag{3.12}$$

$$\frac{d\Psi}{d\tau} = -\sqrt{3}Q\Psi + k\Psi\left(\sqrt{2}\Phi + \sqrt{3/2}a_2 Q\right) - \Psi\chi \tag{3.13}$$

$$\frac{dy}{d\tau} = -\sqrt{3}Qy - \sqrt{1/3c^2}(1-Q^2) - y\chi \tag{3.14}$$

$$\frac{dQ}{d\tau} = \sqrt{1/3}(1-Q^2)(Qy - \tilde{q}) \tag{3.15}$$

$$f(\Phi, \Psi, y, Q) = 1 - c^2y^2 - \Psi^2 - \Phi^2 = 0 \tag{3.16}$$

Where, following [27], we have defined $\chi = \frac{\dot{D}}{D^2}$ and $\tilde{q} = qQ^2$ to make expressing the above equations easier. We are only going to consider certain parameter values. Namely $a_1 = 1$, $a_3 = 0$, $a_2 < 0$. The question of periodic orbits can be addressed by looking at the $Q = \pm 1$ invariant sets, though there is symmetry between these two sets that we will mention later.

In paper [27] the equilibrium points of this system are separated into three categories based upon whether $Q^2 < 1$, or $Q = \pm 1$. We will summarize what happens in the $Q^2 < 1$ and $Q = -1$ cases before we move on to the more interesting case which includes the existence of periodic orbits. The equilibrium points in the $Q^2 < 1$ invariant set correspond to Vacuum Kantowski-Sachs solutions and consists of the points:

$$KS_{vac_1} = \left(0, 0, \frac{1}{c}, 2c\right)$$
$$KS_{vac_2} = \left(0, 0, -\frac{1}{c}, -2c\right)$$

For these equilibrium points, the deceleration parameter q and the spatial curvature ${}^3R$ are both positive. In the $Q^2 < 1$ invariant set, we can eliminate the y variable locally using the integral shown above in (3.16). So now we have reduced the system to three variables. The eigenvalues of the system are below, where the δ determines whether or not they are in the first or second vacuum points above, with $\delta = 1$ referring to KS_{vac_1} and $\delta = -1$ referring to KS_{vac_2}:

$$\frac{\delta\sqrt{3}(1 + 2c^2)}{3c}, \qquad \frac{\delta\sqrt{3}(1 - 4c^2)}{3c} \quad [\times 2]$$

The next two sets of equilibrium points can actually be discussed together since all the points in $Q = 1$ are analogous to the equilibrium points in the $Q = -1$ invariant set, meaning that the same signs exist where the relevant coordinates have the opposite sign. We will focus on the $Q = 1$ for simplicity (there will be no difference in the sign of the deceleration parameter because we have defined $q = \frac{a\ddot{a}}{\dot{a}^2}$).

In the positive space ($Q = 1$), there exists points that lie on the boundary of the phase space and they are the parameterized equilibrium points $C^{\pm}$, and the coordinates for C^{+} are shown below. We are going to follow the same format as in

[27] and refer to points that are in the $Q = 1$ invariant set with a "+" subscript (and similarly with a negative subscript for the ones in the $Q = -1$ invariant set):

$$C^{+} = \left(0, cos(u), \frac{1}{c} sin(u), 1\right), \quad u \in [-\pi, \pi]$$

Using the same technique of eliminating the y variable using the first integral, we can write the eigenvalues of the resulting 3D system:

$$0, \qquad \sqrt{3} - \sqrt{2} k cos(u), \qquad \frac{2\sqrt{3}(2c - |sin(u)|)}{3c}$$

As we noted, these equilibria lie on the boundary of the phase space (which is essentially a 4D sphere) and so it is expected that one of the eigenvalues is zero since the eigenvalues are not strictly independent of each other. The stability of these equilibrium points on the boundary of the phase space depends on the aether parameter a_2, c, k and Φ. For various combinations of these, the points in C^{+} are mostly sources but for some specific combinations of k and c we can achieve some different behavior. The full stability is is shown in [27].

The next two points that we mention in passing are the isotropic equilibrium points:

$$FR^{+}_{\delta} = \left(\frac{-2\sqrt{3}k^2 a_2 + \delta\sqrt{6}K}{3(2 + k^2 a_2^2)}, \frac{2\sqrt{6}k + \delta\sqrt{3K}k a_2}{3(2 + k^2 a_2^2)}, 0, 1\right)$$

where $K = 4k^2\left(\frac{3}{2k^2} + \frac{3a_2^2}{4} - 1\right)$. There are some existence conditions on these two points. The important details are that they are zero curvature and when a scalar field is included, as it is here, these are the FLRW (Friedmann-Lemaitre-Robertson Walker) solutions. The deceleration parameter is $q = \sqrt{6}k\left(\Psi_{eq} - \frac{1}{\sqrt{6}k}\right)$ and then the eigenvalues are conveniently written as:

$$\sqrt{2}k\left(\Psi_{eq} - \frac{3}{\sqrt{6}k}\right) \ [\times 2] \qquad 2\sqrt{2}k\left(\Psi_{eq} - \frac{1}{\sqrt{6}k}\right)$$

So when $q < 0$ and the points are inflationary, all the eigenvalues will be negative since if $\Psi_{eq} < \frac{1}{\sqrt{6}k}$ then $\Psi_{eq} < \frac{3}{\sqrt{6}k}$ is also true. Obviously, if $\frac{1}{\sqrt{6}k} < \Psi_{eq} < \frac{3}{\sqrt{6}k}$ then we have two negative eigenvalues and one positive (and $q > 0$). Lastly, we can have $\Psi_{eq} > \frac{3}{\sqrt{6}k}$ and this is not inflationary.

This last pair of points, neglecting the ones in the $Q = -1$ invariant set, are the most interesting ones and will be the subject of most of the investigation and discussion for this case and Case III.

To investigate the periodic orbits, we want to look at the Bianchi type I equilibrium points of the form:

$$BI_{\delta}^{+} = \left(\frac{-\sqrt{3}a_2}{2}, \frac{\sqrt{6}}{2k}, \frac{\delta\sqrt{-K}}{2kc}, 1 \right)$$

where $K = 4k^2\left(\frac{3}{2k^2} + \frac{3a_2^2}{4} - 1\right) < 0$ as above. We also note that these points only exist for $K < 0$ and $a_2 < 0$. The superscript '+' means that we are in the $Q = 1$ invariant set and the parameter $\delta = \pm 1$. We can calculate $\nabla f\big|_{BI_{\delta}^{+}}$ and eliminate y from the dynamical system using the first integral. The eigenvalues of the resulting 3D system are then:

$$\frac{\sqrt{3}}{3kc}\left(4kc - \delta\sqrt{-K}\right) \ , \ \pm\frac{\sqrt{6}a_2\sqrt{-K}}{4}i$$

We note that the pure imaginary eigenvalues at this point span the invariant set $Q = 1$ and further reduce the system to a two-dimensional system in terms of Φ and Ψ. We then translate the equilbrium point to the origin and change to polar coordinates [27]:

$$rcos(\theta) = \frac{1}{\sqrt{2}k(3a_2^2 - 4)}\left(\Phi + \frac{\sqrt{3}a_2}{2}\right)$$

$$rsin(\theta) = \frac{3a_2}{2k\sqrt{-K}(3a_2^2 - 4)}\left(\Phi + \frac{\sqrt{3}a_2}{2}\right) + \frac{1}{2\sqrt{-2K}}\left(\Psi - \frac{\sqrt{6}}{2k}\right)$$

Taking derivatives and rearranging leaves us with the following system of differential equations in terms of r and θ:

$$r' = \frac{-kr^2}{\sqrt{-K}}\left(Ka_2 sin\theta - 2\sqrt{-2K}cos\theta\right)\left(\left(2\sqrt{6}k(3a_2^2 - 4)cos\theta\right)r + 3a_2\right) \tag{3.17}$$

$$\theta' = \frac{-\sqrt{-K}}{2\sqrt{6}}\left(\left(2\sqrt{6}k(3a_2^2 - 4)cos\theta\right)r + 3a_2\right) \tag{3.18}$$

Since the above represents a full view of the potential non-linear centers that we found in BI^{+}_{δ}, rather than just a linearization, the goal is to integrate $\frac{dr}{d\theta}$ around one rotation to see whether it is actually a closed orbit (i.e. higher order). Meaning that if the linearization gave a pure imaginary eigenvalue, we wanted to see if it was truely a closed orbit when we included the $\Phi^2, \Phi^3, \Psi^2, \Psi^3$ terms, for example. Note that this is not a rigorous proof of the existence of closed orbits but a way to provide further evidence of such closed orbits. If the integral is zero, we know that the orbit is closed, and if not then we know that some higher order terms are causing an instability.

Since the RHS for both of the above equations contain the same factor, we can eliminate it in the calculation of $\frac{dr}{d\theta}$. The resulting differential equation is:

$$\frac{dr}{d\theta} = \frac{2\sqrt{6}kr^2}{K}\left(Ka_2 sin\theta - 2\sqrt{-2K}cos\theta\right)$$

This is separable so the solution can be written as:

$$r(\theta) = \left(\frac{1}{r_0} - 2\sqrt{6}ka_2(cos\theta - 1) + \frac{8\sqrt{3}k}{\sqrt{-K}}sin\theta\right)^{-1}$$

where $r(0) = r_0$ is a constant of integration, which would be the solution to the DE at first order. If you were to travel one revolution around the orbit, the second and third terms are zero and so the radius at 2π is equal to the initial radius $\frac{1}{r_0}$. This consequently defines a family of periodic orbits. From the equation for θ', we can also see that the linear term is negative, since these points only exist for $a_2 < 0$, and so the periodic orbits are rotating in a counter-clockwise direction. This part of the analysis is only for the two completely imaginary eigenvalues. The sign of the other eigenvalue for the Bianchi type I equilibrium points depends on the sign of the term $4kc - \delta\sqrt{-K}$. Based on our definition of K from earlier we have:

$$\begin{aligned} K + (4kc)^2 &< 0 \\ \Rightarrow 4c^2 + \frac{3}{2k^2} + \frac{3a_2^2}{4} - 1 &< 0 \\ \Rightarrow 4c^2 + \frac{3}{2k^2} + \frac{3a_2^2}{4} &< 1 \end{aligned}$$

What this essentially shows us is a relationship between a_2, the scalar field parameter k, and the aether parameter, c, in order to have an infinite family of stable, periodic

orbits. Another thing to note is that for all of the Bianchi type I points, the deceleration parameter is $q = 2$, so these points are non-inflationary.

Next we shall present a short summary of Case II, and leave the comparison between the various models for the discussion section. Not including the parameterized equilibrium points $C^{\pm}$, there are 10 other points and these can be broken into 3 different invariant sets, namely, $Q^2 < 1$ and $Q = \pm 1$. The vacuum Kantowski-Sachs solutions exists in the $Q^2 < 1$ invariant set and are both non-inflationary. They only exist when the aether parameter $c < \frac{1}{2}$. One of them is a sink and the other is a source.

Moving to the $Q = 1$ invariant set, there are three main categories of points; The Kasner points, the isotropic points and the Bianchi type I points. Starting with the Kasner Points, there are two rings of points, parameterized by u in our calculations above. There are varying ranges of parameters for which the Kasner points changes stability. For $k^2 < \frac{3}{2}$ they are all sources in the reduced phase space, and either remain sources or become a mixture of sources and saddles in the 3D phase space. If $k^2 > \frac{3}{2}$ then they are mostly sources. This is also true in the 3D phase space but we can also have ranges of the parameter k for which some of these points become saddles. These points are called "Kasner-like" after the early 20th century mathematician Edward Kasner. The Kasner metric describes an anisotropic universe without matter and is an exact solution to Einstein's General Relativity [17]. From the coordinates of the equilibrium points in these Kasner Points, we can see that the scalar field variable Φ is zero, but that the variable associated with its derivative, Ψ, as well as y and Q, the variables having to do with the shear and expansion terms, are non-zero for certain values of u. From the definition of q (which we discuss in more detail in Case III, also see [27]), we can see that these Kasner Points are non-inflationary. In fact, for the Kasner points we have $\tilde{q} \equiv qQ^2 = 2$.

The next set of points are the isotropic points. As the name implies, these are akin to the FLRW models with a scalar field. FR^{+}_{-} exists in the physical phase space if $k^2 \geq \frac{3}{2}$ and $a_2 < 0$, $K > 0$. For these Isotropic Points, there is a convenient way of

representing the eigenvalues and deceleration parameter in terms of the equilibrium value Ψ_{eq} at these points; for $\Psi_{eq} < \frac{1}{\sqrt{6}k}$ we have inflationary sinks, for $\frac{1}{\sqrt{6}k} < \Psi_{eq} < \frac{3}{\sqrt{6}k}$ we have non-inflationary saddles and, finally, if we have $\Psi_{eq} > \frac{3}{\sqrt{6}k}$ then the points are non-inflationary sources.

The final set of points are the Bianchi type I Points around which we find the periodic orbits (i.e. these Bianchi type I points are non-linear centers). These arise because we find eigenvalues that are pure imaginary with zero real part and our reparameterization of these points demonstrates that these periodic orbits can exist for small values of the integration constant r_0. There is also a dependence on the parameters a_2 and k but these only affect, for instance, how quickly we travel one complete circular orbit. As mentioned previously, similar arguments can be made for all the points in the $Q = -1$ invariant set. There are some differences, however, such as FR_- existing in the physical phase space both for the conditions we gave for FR_+^+ as well as for the case $k^2 \leq \frac{3}{2}$. More generally, the stable and unstable manifolds in the $Q = 1$ switch stability in the $Q = -1$ invariant sets. As dicussed in [27] switching between these invariant sets effectively changes the sign of the eigenvalues. The saddles also reverse the number of stable and unstable manifolds when the equilibrium points are translated between the $Q = \pm 1$ invariant sets. We can summarize all of the equilibrium points and their properties in the following table:

ID	Coords. $\{\Phi, \Psi, y, Q\}$	Decel.	Curv.	Eigenvalues
KS_δ	$0, 0, \frac{\delta}{c}, 2\delta c$	+	+	$\frac{\sqrt{3}k(1+2c^2)}{3c}, \frac{\sqrt{3}k(1-4c^2)}{3c}$ $[\times 2]$
C^+	$0, cos(u), \frac{sin(u)}{c}, 1$	+	0	$0, \sqrt{3} - \sqrt{2}kcos(u), \frac{2\sqrt{3}(2c-\lvert sin(u)\rvert)}{c}$
C^-	$0, -cos(u), -\frac{sin(u)}{c}, -1$	+	0	$0, -\sqrt{3} + \sqrt{2}kcos(u), -\frac{2\sqrt{3}(2c-\lvert sin(u)\rvert)}{c}$
FR_δ^+	$\left(\frac{-2\sqrt{3}k^2a_2+\delta\sqrt{6}K}{3(2+k^2a_2^2)}, \frac{2\sqrt{6}k+\delta\sqrt{3K}ka_2}{3(2+k^2a_2^2)}, 0, 1\right)$	-	0	$2\sqrt{2}k(\Psi_{eq} - \frac{1}{\sqrt{6}k}), \sqrt{2}k(\Psi_{eq} - \frac{3}{\sqrt{6}k})$ $[x2]$
FR_δ^-	$\left(\frac{2\sqrt{3}k^2a_2+\delta\sqrt{6}K}{3(2+k^2a_2^2)}, \frac{-2\sqrt{6}k+\delta\sqrt{3K}ka_2}{3(2+k^2a_2^2)}, 0, -1\right)$	-	0	$2\sqrt{2}k(\Psi_{eq} - \frac{1}{\sqrt{6}k}), \sqrt{2}k(\Psi_{eq} - \frac{3}{\sqrt{6}k})$ $[x2]$
BI_δ^+	$-\frac{\sqrt{3}a_2}{2}, \frac{\sqrt{6}}{2k}, \frac{\delta\sqrt{-K}}{2kc}, 1$	+	0	$\frac{\sqrt{3}}{3kc}(4kc - \delta\sqrt{-K}), \pm\frac{a_2\sqrt{-6K}}{4}i$
BI_δ^-	$\frac{\sqrt{3}a_2}{2}, -\frac{\sqrt{6}}{2k}, \frac{\delta\sqrt{-K}}{2kc}, -1$	+	0	$\frac{\sqrt{3}}{3kc}(4kc - \delta\sqrt{-K}), \pm\frac{a_2\sqrt{-6K}}{4}i$

Table 3.3: Equilibria for Case II

Note that there are some slight differences between the invariant sets that are not explicitly shown in the above table. First, there are a couple differences between where the various equilibria exist, in there respective invariant sets. For example, for the Bianchi Type I points, we have $a_2 < 0$ for $Q = 1$ but $a_2 > 0$ if $Q = -1$ if these points are to exist. In C^+ and C^- we have that for certain parameter ranges ($k^2 > \frac{3}{2}$ and $c < \frac{1}{2}$) the points are saddles and have the same number of stable manifolds in both $Q = \pm 1$. The Isotropic Equilibria have similar existence conditions to the Bianchi Type I points; $a_2 < 0$ and $a_2 > 0$ for the $Q = 1$ and $Q = -1$ invariant sets, respectively. Lastly, the Isotropic Equilibria have a_2 parameters with different signs in the case when you are discussing the case when they are either an infaltionary sink or source in the $Q = 1$ and $Q = -1$ cases, respectively.

As in the previous case, we can also present some numerics of the system to illustrate the analytical behaviour that we have found. Since this is a 4-dimensional system, it is difficult to show the full orbits since it would require the use of an animation (or something similar). Following a similar method to what we used when analyzing the model algebraically, we can look into the behaviour in certain invariant sets. For instance, $Q = 1$. The other variables can then be represented fully by a numerical solution in 3D. In picking the initial conditions, we need to keep in mind that $\Phi > 0$ and y can be completely determined by the constraint imposed by the first integral (3.16). In the $Q = 1$ (and $Q = -1$, though flipped to the negative Ψ quadrant) we can see the formation of the periodic orbit. Below we present a plot with $c = 0.25$ and $c = 1$. Since c is just a scale variable for the elipse represented by the first integral (3.16), the only difference is the stretch of the phase plane. The initial conditions are where the two colors, the backward and forward time evolved solutions, meet. The cyan color represents the backward solution while the pink color represents the forward solution. For example, we can see that the Kasner points C^+ which we have identified as mostly sources in the work above, are shown as sources by the cyan solutions tending to them in the past. In terms of the axes, Ψ is represented by the green axis, Φ by the red axis and y by the magenta axis.

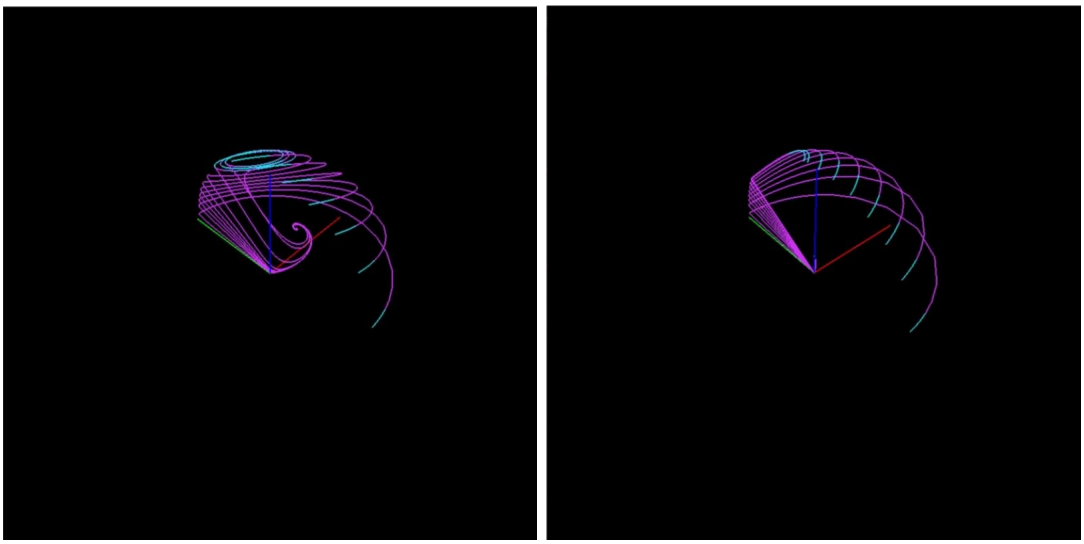

Figure 3.7: $k = 2, a_2 = -0.5, c = 1$ and $k = 2, a_2 = -0.5, c = 1$

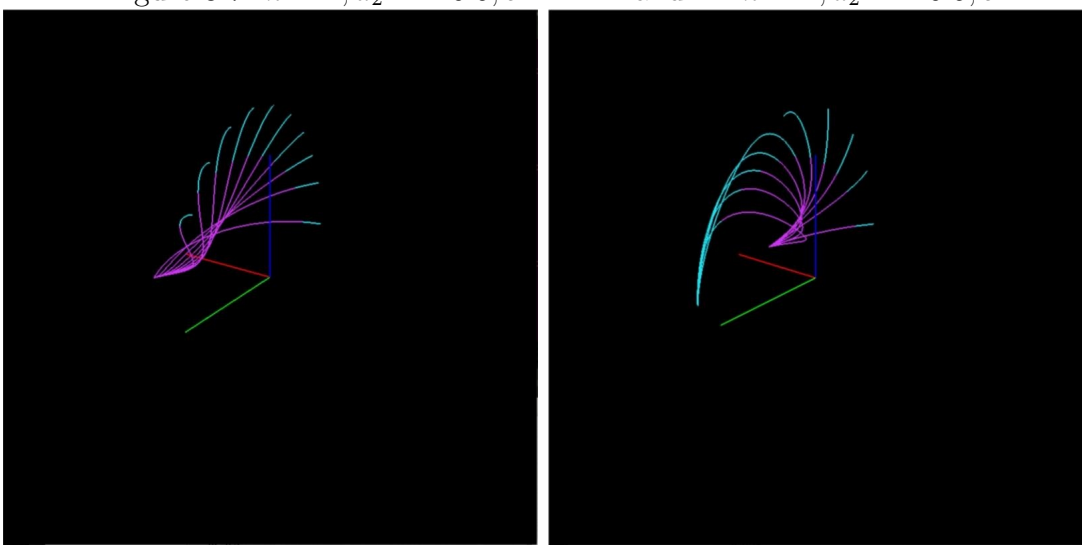

Figure 3.8: $k = 0.5, a_2 = 0.5, c = 0.75$ and $k = 2.1, a_2 = -1.5, c = 0.75$

3.3 Case III - Shear, Constant-Plus-Exponential Potential

In this last case, we are going to be including the coupling term, and a constant-plus-exponential potential in the form $V = e^{-2k\phi} + a_2\theta e^{-k\phi} + \Lambda$, so we have let $a_1 = 1$ and $a_3 = 0$ from the original model [27]. In this case we are going to fully work out the details since we omitted many of the calculations in the previous case. Fully fleshing out the details will also allow us to see the complete impact on the dynamical system due to this addition of the cosmological constant into the potential. In

the Kantowski-Sachs framework, the metric is (2.4) where $a(t)$ and $b(t)$ are arbitrary functions of time.

The vorticity and the acceleration of the aether vector are zero. The covariant derivative of the aether vector, the expansion scalar, shear tensor and shear scalar, as well as the effective energy density ρ^U, isotropic pressure p^U, energy flux q_a^U and anisotropic stress ${\pi^a}_b{}^U$ due to the aether field (note the superscript U), can be found in [27]. The energy momentum tensors due to the aether field and scalar field are as they are defined in Case II. As before, the Einstein field equations reduce to:

$$
\begin{aligned}
0 &= -\frac{1}{3}(1+c_\theta)\theta^2 + 3(1-2c_\sigma)\sigma_+^2 - {}^3R + 8\pi G\rho^M \\
0 &= -(1+c_\theta)\dot{\theta} - \frac{1}{3}(1+c_\theta)\theta^2 - 6(1-2c_\sigma)\sigma_+^2 - \frac{8\pi G}{2}(\rho^M + 3p^M) \\
0 &= (1+2c_\sigma)\dot{\sigma_+} + (1-2c_\sigma)\theta\sigma_+ + {}^3R - 8\pi G\pi_+^M
\end{aligned}
$$

The terms in the first and second equations are what will be affected by the change in the potential. The effective energy density, isotropic pressure, energy flux and anisotropic stress due to the scalar field with our new potential are below. These are found by working through all the terms of the energy momentum tensor for the scalar field. For instance, the calculation of ρ^M is shown below:

$$
\begin{aligned}
T_{00}^M &= \rho^M \\
&= \nabla_t\phi\nabla_t\phi - \left(\frac{1}{2}\nabla_t\phi\nabla^t\phi + V\right)g_{00} + \theta V_\theta g_{00} + \dot{V}_\theta h_{00} + (\theta V_{\sigma^2} + \dot{V}_{\sigma^2})\sigma_{00} \\
&= \dot{\phi}^2 - \frac{1}{2}\dot{\phi}^2 + \left(e^{-2k\phi} + a_2\theta e^{-k\phi} + \Lambda\right) + \theta a_2 e^{-k\phi} g_{00} + 0 \\
&= \frac{1}{2}\dot{\phi}^2 + e^{-2k\phi} + \Lambda
\end{aligned}
$$

The full list of terms from the energy momentum tensor are presented below, including the one we just derived for the effective energy density, in matrix form:

$$T^M_{ab} = \begin{pmatrix} \frac{1}{2}\dot{\phi}2 + e^{-2k\phi} + \Lambda & 0 & 0 & 0 \\ 0 & -\frac{1}{2}a^2T & & 0 \\ 0 & 0 & -\frac{1}{2}b^2T & 0 \\ 0 & 0 & & -\frac{1}{2}b^2sin^2(\theta)T \end{pmatrix}$$

where $T = 2a_2k\dot{\phi}e^{-k\phi} - \dot{\phi}^2 + 2\Lambda + 2e^{-2k\phi}$. From this matrix we can get the above mentioned terms and they are:

$$\rho^M = \frac{1}{2}\dot{\phi}^2 + e^{-2k\phi} + \Lambda \tag{3.19}$$

$$p^M = \frac{1}{2}\dot{\phi}^2 - e^{-2k\phi} - ka_2\dot{\phi}e^{-k\phi} - \Lambda \tag{3.20}$$

$$q^M_a = 0 \tag{3.21}$$

$$\pi^M_+ = 0 \tag{3.22}$$

In order to get a complete system similar to that in the previous cases, we need to substitute (3.19, 3.20, 3.21 and 3.22) into the reduced Einstein-aether equations and the first integral, from which we will draw on to give us an idea for new, dimensionless normalized variables. First, we derive the new equation for $\dot{\sigma}_+$:

$$\begin{aligned} 0 &= (2-2c_\sigma)\dot{\sigma}_+ + (1-2c_\sigma)\theta\sigma_+ + \frac{1}{3b(t)^2} \\ \Rightarrow\ \dot{\sigma}_+ &= -\theta\sigma_+ - \frac{1}{3(1-2c_\sigma)}\left(-\frac{1}{3}(1+c_\theta)\theta^2 + 3(1-2c_\sigma)\sigma_+^2 + 8\pi G\left(\frac{1}{2}\dot{\phi}^2 + e^{-2k\phi} + \Lambda\right)\right) \\ &= -\theta\sigma_+ - \sigma_+^2 - \frac{1}{3c^2}\left(-\frac{1}{3}\theta^2 + \frac{1}{2}\dot{\phi}^2 + e^{-2k\phi} + \Lambda\right) \end{aligned}$$

The full list of Einstein's equations with (3.19, 3.20, 3.21 and 3.22) are then:

$$\dot{\theta} = -\frac{1}{3}\theta^2 - 6c^2\sigma_+^2 - \psi^2 + e^{-2k\phi} + \frac{3}{2}ka_2\dot{\phi}e^{-k\phi} + \Lambda \tag{3.23}$$

$$\dot{\sigma}_+ = -\theta\sigma_+ - \sigma_+^2 + \frac{1}{3c^2}\left(\frac{1}{3}\theta^2 - \frac{1}{2}\psi^2 - e^{-2k\phi} - \Lambda\right) \tag{3.24}$$

$$\dot{\phi} = \psi \tag{3.25}$$

$$\dot{\psi} = -\theta\psi + 2ke^{-2k\phi} + a_2k\theta e^{-k\phi} \tag{3.26}$$

The first integral can be computed from the first reduced Einstein field equation on page 31 along with (3.19-3.22), and is:

$$\frac{1}{b^2(1+c_\theta)} = -\frac{1}{3}\theta^2 + 3c^2\sigma_+^2 + \frac{1}{2}\psi^2 + e^{-2k\phi} + \Lambda \tag{3.27}$$

We shall assume $\Lambda > 0$. As before, the first integral gives us an idea of how to rescale the variables. We are also going to redefine the time coordinate as well so that we can ensure that the system will be bounded - this allows for a much cleaner analysis. Again, we have $D = \sqrt{\frac{1}{1+c_\theta}\frac{1}{b^2} + \frac{1}{3}\theta^2}$, which from (3.27) is strictly positive and as before we have $\frac{d\tau}{dt} = D$. The bounded, new variables are then:

$$\Phi = \frac{e^{-k\phi}}{D}, \qquad \Psi = \frac{\psi}{\sqrt{2}D}, \qquad y = \frac{\sqrt{3}\sigma_+}{D}, \qquad Q = \frac{\theta}{\sqrt{3}D}, \qquad x = \frac{\sqrt{\Lambda}}{D}$$

Now with these new variables we can derive the new dimension normalized equations. We again define $\chi = \frac{\dot{D}}{D^2}$. This is the same as in Case II but here we will show the full calculation of this term. Now we can derive the normalized equations and we show one calculation below as an example. The equation for $y' = \frac{dy}{d\tau} = \frac{dy}{dt}\frac{dt}{d\tau}$ is:

$$\begin{aligned} y &= \frac{\sqrt{3}\sigma_+}{D} \\ \Rightarrow y' &= \frac{\sqrt{3}\dot{\sigma_+}}{D^2} - \frac{\sqrt{3}\sigma_+}{D}\frac{\dot{D}}{D^2} \\ &= \frac{\sqrt{3}\dot{\sigma_+}}{D^2} - y\chi \\ &= \sqrt{3}yQ - \frac{1}{\sqrt{3}}y^2 + \frac{1}{\sqrt{3}c^2}\left(Q^2 - \Psi^2 - \Phi^2 - x^2\right) - y\chi \end{aligned}$$

We note that an extra factor of $\frac{1}{D}$ comes from the fact that we are now considering overdots to represent differentiation with respect to the new time variable τ. The remaining equations are:

$$\frac{d\Phi}{d\tau} = -\Phi\left(\sqrt{2}k\Psi + \chi\right) \tag{3.28}$$

$$\frac{d\Psi}{d\tau} = -\sqrt{3}\Psi Q + k\Phi\left(\sqrt{2}\Phi + \sqrt{\frac{3}{2}}a_2 Q\right) - \Psi\chi \tag{3.29}$$

$$\frac{dy}{d\tau} = -\sqrt{3}yQ + \frac{1}{\sqrt{3}c^2}\left(Q^2 - \Psi^2 - \Phi^2 - x^2 - c^2y^2\right) - y\chi \tag{3.30}$$

$$\frac{dQ}{d\tau} = \frac{1}{\sqrt{3}}\left(1 - Q^2\right)(Qy - \tilde{q}) \tag{3.31}$$

$$\frac{dx}{d\tau} = -x\chi \tag{3.32}$$

with first integral

$$f(\Phi, \Psi, y, Q, x) = 1 - c^2y^2 - \Phi^2 - \Psi^2 - x^2 = 0$$

As we mentioned above, the first four equations and the first integral are very similar to what we encountered in Case II. The major difference is that the $1 - Q^2$ terms now implicitly contain the new variable x. The calculation for χ is:

$$\begin{aligned}
\chi &= \frac{\dot{D}}{D^2} \\
&= \frac{1}{2D^3}\left(\frac{1}{1+c_\theta}\frac{1}{b^2} + \frac{\theta^2}{3}\right)' \\
&= \frac{1}{2D^3}\left(-\frac{\theta^2}{3} + 3c^2\sigma_+^2 + \frac{\psi^2}{2} + e^{-2k\phi} + \frac{\theta^2}{3} - \Lambda\right)' \\
&= \frac{1}{2D^3}\left(6c^2\sigma_+\dot{\sigma_+} + \frac{1}{2}\psi\dot{\psi} - 2k\psi e^{-2k\phi}\right) \\
&= \sqrt{3}c^2y\frac{\dot{\sigma_+}}{D^2} + \frac{1}{\sqrt{2}}\Psi\frac{\dot{\psi}}{D^2} - \sqrt{2}k\Psi\Phi^2 \\
&= \sqrt{3}c^2y\left(-yQ + \left(\frac{1}{3c^2}\left(Q^2 - \Psi^2 - \Phi^2 - c^2y^2 - x^2\right)\right)\right) + \frac{1}{\sqrt{2}}\Psi(-\sqrt{6}\Psi Q + 2k\Phi^2 \\
&\qquad + \sqrt{3}a_2kQ\Phi) - \sqrt{2}k\Psi\Phi^2 \\
&= \frac{1}{\sqrt{3}}y(Q^2 - 1) - \frac{1}{\sqrt{3}}Q\left(3c^2y^2 + 3\Psi^2 + \frac{3}{\sqrt{2}}a_2k\Psi\Phi\right) \\
&= \frac{1}{\sqrt{3}}\left(y\left(Q^2 - 1\right) - Q\left(\tilde{q_\Lambda} + 1\right)\right)
\end{aligned}$$

where $\tilde{q} = 2c^2y^2 + 2\Psi^2 - \Phi^2 - x^2 + \frac{3}{\sqrt{2}}a_2k\Phi\Psi$.

We want to find solutions for which $x \neq 0$, since if $x = 0$ then our analysis will look identical to Case II. We can again classify the new equilibria based on which invariant set they inhabit; i.e., $Q = \pm 1$. We find that there are no new equilibria in Case III that are in the $Q^2 < 1$ invariant set. If $\chi = 0$, then by examining our new equations (3.28-3.32) either $\Psi = 0$ or $\Phi = 0$ (or both are equal to zero). We will choose $\Phi = 0$ first. Substituting this and $Q = \pm 1$ into the equations results in $y = 0$ and $\Psi = 0$. If instead we choose $\Psi = 0$, then we get one solution for each choice of $Q = \pm 1$. The entire list of new equilibria for the $x \neq 0$ case is listed below (note that the constraint equation is satisfied for all of the coordinate values of the equilibria and can be reduced to $0 = 1 - c^2y^2 - \Phi^2 - \Psi^2 - x^2 = 1 - \Phi^2 - x^2$ since $y = \Psi = 0$ for the equilibrium points for which $\chi \neq 0$ we are considering here).

ID	Φ	Ψ	y	Q	x (only $x \neq 0$ cases)
a	0	0	0	1	1
c	0	0	0	-1	1
e	$-\frac{\sqrt{3}}{2}a_2$	0	0	1	$\sqrt{1-\frac{3}{4}a_2^2}$
g	$\frac{\sqrt{3}}{2}a_2$	0	0	-1	$\sqrt{1-\frac{3}{4}a_2^2}$

Table 3.4: New Equilibria for Case III

Many of the equilibria that can be algebraically solved for are not physically realistic so we do not include them in above table. There are also constraints on a_2 for point e) to exist. From the coordinate for Φ, we must have $a_2 < 0$ since Φ is defined in terms of the exponential from the scalar field potential. The coordinate for x must also be positive because of the way it is defined in the system above. The end result is that $-\frac{2}{\sqrt{3}} < a_2 < 0$ for point e) to exist. For point g), we must assume $a_2 > 0$ for the Φ coordinate to be valid and so this coupled with the restriction for the x coordinate means we must have $0 < a_2 < \frac{2}{\sqrt{3}}$.

Since the system is 5D with one constraint and highly non-linear, we are not going to show the general Jacobian since it is excessively long and complicated. In fact,

since $x \neq 0$ in a neighborhood of the above equilibrium points, we can use the first integral $x^2 = 1 - c^2y^2 - \Phi^2 - \Psi^2$ to locally eliminate x. Once we evaluate the Jacobian at each of the equilibrium points, the expressions become relatively simple so we can show them below. The Jacobian and eigenvalues for point a) are:

$$J_a = \begin{pmatrix} 0 & 0 & 0 & 0 \\ \frac{\sqrt{6}}{2}ka_2 & -\sqrt{3} & 0 & 0 \\ 0 & 0 & -\sqrt{3} & \frac{2}{\sqrt{3}c^2} \\ 0 & 0 & 0 & -\frac{2}{\sqrt{3}} \end{pmatrix}, \qquad Eigenvalues = \begin{pmatrix} 0 \\ -\frac{2}{\sqrt{3}} \\ -\sqrt{3} \\ -\sqrt{3} \end{pmatrix}$$

The Jacobian and eigenvalues for e) are:

$$J_e = \begin{pmatrix} 0 & \frac{\sqrt{6}}{8}ka_2(3a_2^2+4) & 0 & 0 \\ -\frac{\sqrt{6}}{2}ka_2 & -\sqrt{3} & 0 & -\frac{3\sqrt{2}}{4}ka_2^2 \\ 0 & 0 & -\sqrt{3} & \frac{2}{\sqrt{3}c^2} \\ 0 & 0 & 0 & -\frac{2}{\sqrt{3}} \end{pmatrix}$$

$$Eigenvalues = \begin{pmatrix} -\frac{\sqrt{3}}{2} + \frac{1}{4}\sqrt{-18a_2^4 4k^2 - 24a_2^2k^2 + 12} \\ -\frac{\sqrt{3}}{2} - \frac{1}{4}\sqrt{-18a_2^4 4k^2 - 24a_2^2k^2 + 12} \\ -\sqrt{3} \\ -\frac{2}{\sqrt{3}} \end{pmatrix}$$

The eigenvalues for c) are exactly that of a) except with the signs switched, and a similar thing happens for points e) and g). For the given range of the parameter a_2, the first eigenvalue for point e) will always be negative (since the term under the square root will be < 12 for all possible values of a_2 and k) and by inspection, the second eigenvalue must also always be negative and so point e) is a sink. We also want to determine the local behaviour around points $a), c)$ with zero eigenvalue. Wiggins' [28] method for determining stability of a center manifold as used in Case I can again help us to clarify the dynamics at this point. We will show the calculation for point a) below, but a similar calculation can be done for c. Note that this method is only valid if all of the other eigenvalues are non-zero, which they are for each of these cases.

The zero eigenvalue for point a) occurs in the Φ direction, so we need to expand the other variables around that. We let:

$$h = \begin{bmatrix} \Psi \\ y \\ Q \\ x \end{bmatrix} = \begin{bmatrix} \alpha_1\Phi^2 + \alpha_2\Phi^3 + ... \\ b_1\Phi^2 + b_2\Phi^3 + ... \\ c_1\Phi^2 + c_2\Phi^3 + ... \\ d_1\Phi^2 + d_2\Phi^3 + ... \end{bmatrix}$$

$$\dot{x} = Ax + f(x, h(x))$$
$$\dot{y} = Bh(x) + g(x, h(x))$$

where A is a matrix with the linear terms of Φ from all the equations, B is a matrix of the linear terms of the other variables encoded in a 4×4 diagonal matrix. f is all the non-linear terms from the Φ equation and g is the non-linear terms from the other equations. This is the same method as before, although there are some linear terms that need to be accounted for that we did not have to take into consideration last time. The algebra is complicated so we will omit it here. The result is a system of equations for α_1, b_1, c_1, d_1 that we can solve and substitute back into the rescaled equation for Φ so that we can determine the behaviour. We only need the system up to second order and it is:

$$\begin{aligned} \Phi^2\left(\sqrt{3}\alpha_1 - k\sqrt{2}\right) &= 0 \\ \Phi^2\left(\sqrt{3}b_1 + \frac{1}{\sqrt{3}c^2} - \frac{2c_1}{\sqrt{3}c^2} + \frac{2d_1}{\sqrt{3}c^2}\right) &= 0 \\ \frac{2c_1}{\sqrt{3}}\Phi^2 &= 0 \\ \Phi^2\left(\frac{2d_1}{\sqrt{3}} + \frac{1}{\sqrt{3}}\right) &= 0 \end{aligned}$$

Solving this gives us $\alpha_1 = \sqrt{\frac{2}{3}}k, b_1 = 0, c_1 = 0, d_1 = -\frac{1}{2}$. We take these values and substitute them back into h, then substitute back into the equation for Φ' to obtain

$$\Phi' = -\frac{2k^2}{\sqrt{3}}\Phi^3 + \mathcal{O}(\Phi^4) \tag{3.33}$$

Given that the dynamics in a neighborhood of the equilibrium point are governed by

this equation, we can see that for sufficiently small Φ (i.e. $\Phi \approx 0$) that the derivative Φ' will be negative. Together with the other negative eigenvalues shown above, we can conclude that this point will be a sink in the full phase space.

We also show some numerical solutions for this case. The periodic orbits from the last case will still be present in the invariant set $x = 0$ in this case. To show some of the dynamics that include the cosmological constant, we consider $x \neq 0$. We will show orbits for a few different combinations of the parameters in a reduced 3D phase space. We will set $Q = 1$ as before. The first set of figures will be in Φ, Ψ and y space (with x eliminated from the constraint) with similar parameters as before. The second set of figures are in Φ, Ψ and x space (with y eliminated with the constraint):

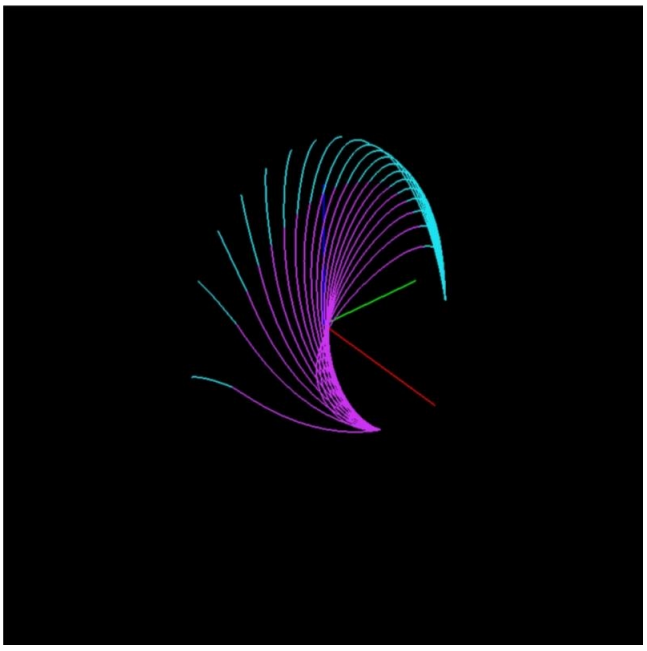

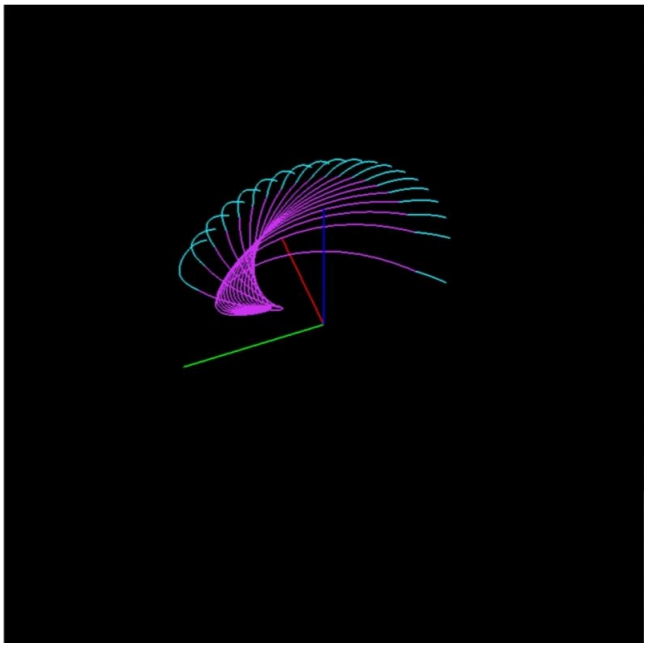

Figure 3.9: $k = 2.1, a_2 = -1.5, c = 0.8$ and $k = 1.2, a_2 = 0.5, c = 0.8$

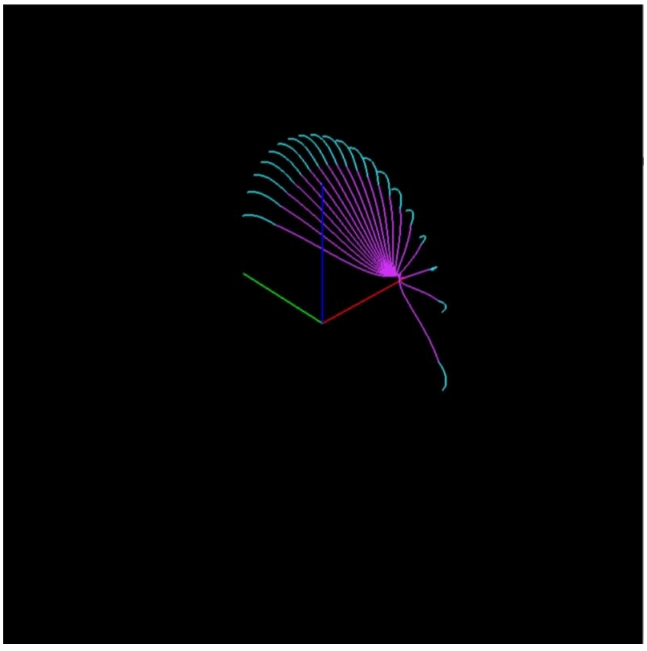

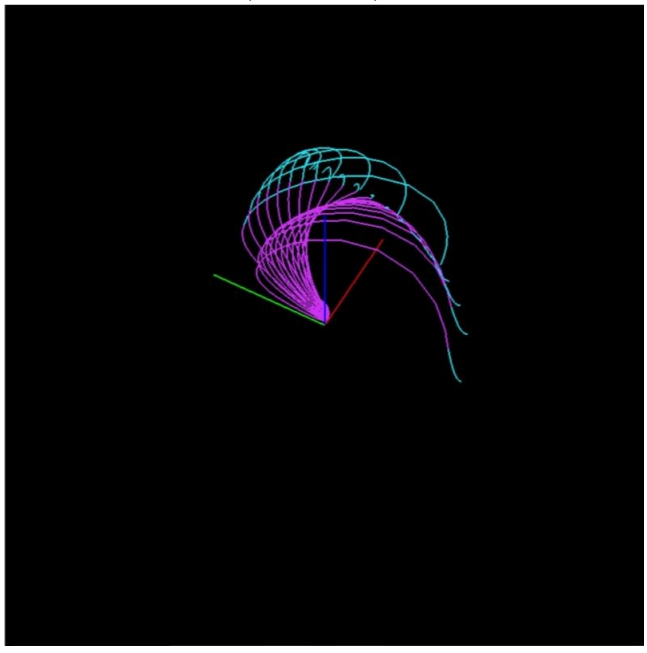

Figure 3.10: $k = 0.1, a_2 = -0.1, c = 0.8$ and $k = 3.5, a_2 = 0, c = 0.8$

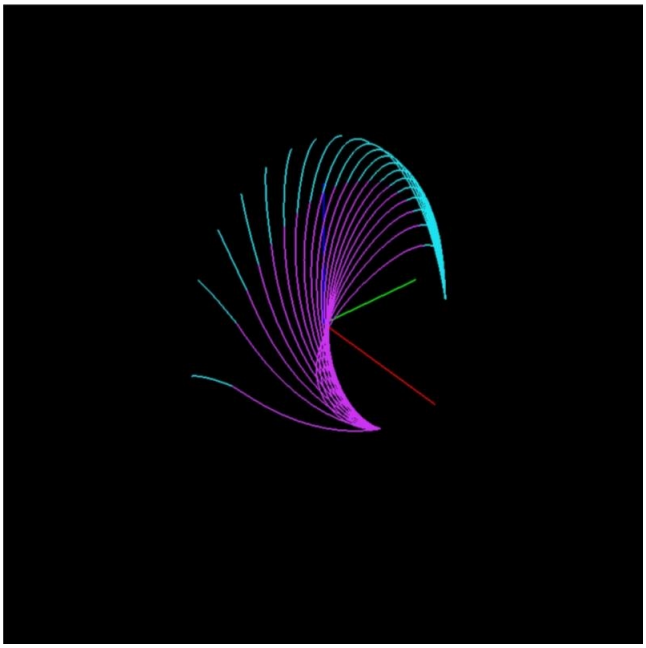

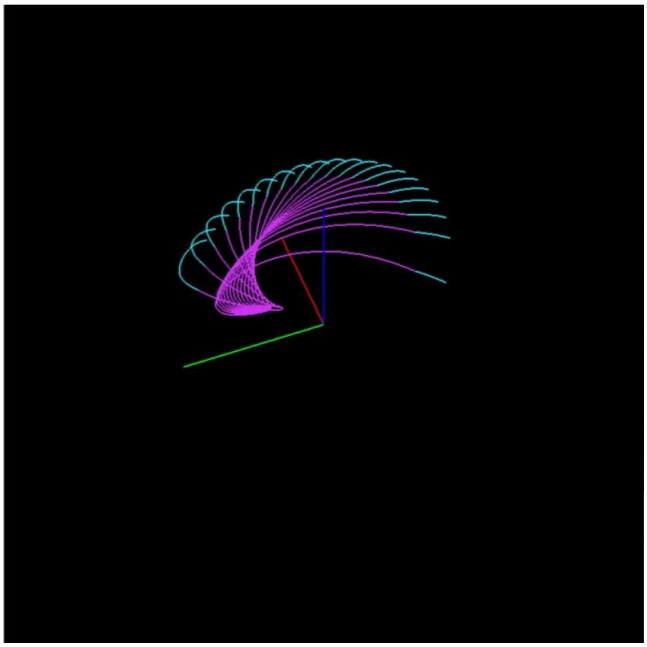

Figure 3.11: $k = 2.1, a_2 = -1.5, c = 0.8$ and $k = 1.2, a_2 = 0.5, c = 0.8$

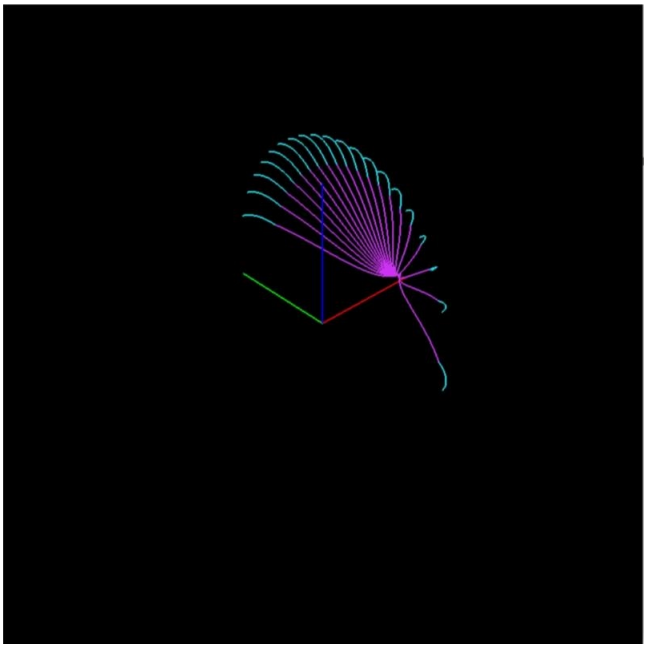

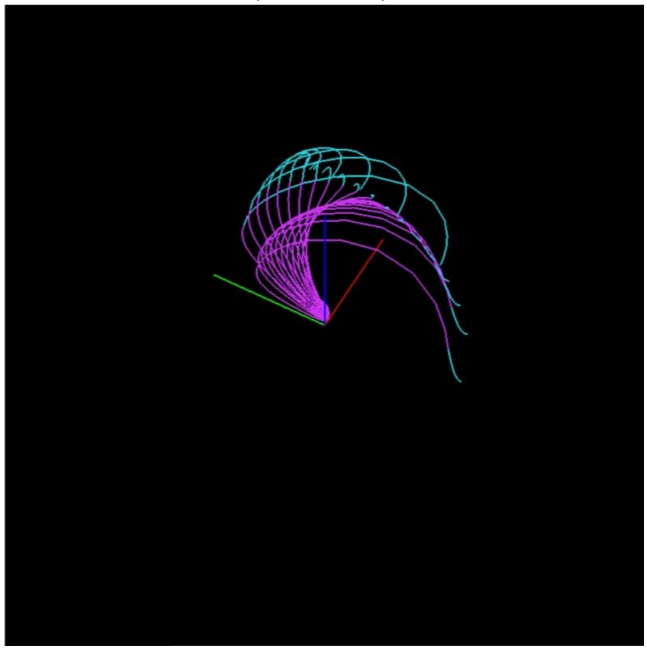

Figure 3.12: $k = 0.1, a_2 = -0.1, c = 0.8$ and $k = 3.5, a_2 = 0, c = 0.8$

Chapter 4

Discussion

In Case I we were able to break up the analysis into two distinct cases, a reduced 2x2 system and a more complete 3x3 system (referred to as Case Ia and Case Ib, respectively). In both Case Ia and Ib, we were not looking at a true Kantowski-Sachs model, but instead a simple single scalar field FLRW cosmology. Case Ib was the same except for the introduction of a cosmological constant. In these models, the scalar field is present at early times, and the late time attractor only had V_0 present and so at late times, the cosmological constant dominated. The corresponding sink had a spatial curvature of 0 and is also inflationary. We also mentioned that point e) is a saddle when $k < \sqrt{3/2}$ with varying numbers of stable and unstable manifolds and this point is inflationary for $k < \sqrt{1/2}$. This point only depends on the scalar field and potential and so the system could evolve close to this state for arbitrarily long periods of time.

Cases II and III are true Kantowski-Sachs models since we began with the KS metric and worked out the resulting dynamical system. These cases include the shear term. In Case II, we see that there are a number of different ranges of the parameters where the system changes behaviour. We found that there are isotropic, expanding and power-law inflationary solutions that are late time attractors. Interestingly enough, we also found that there are an infinite number of periodic orbits and when we adjust the parameter a_2 in these periodic orbits, we can change the 'speed' of revolution around these orbits. The existence of the periodic orbits only depended on the relative magnitude of an integration constant r_0.

There is also a phenomenon called assisted inflation, in which if we have two scalar fields where each of the k_1, k_2 scalar field parameters are too large to separately initiate inflation, the two scalar fields can achieve inflation by means of an effective scalar

field parameter where the condition for inflation is $\frac{1}{K^2} = \frac{1}{k_1^2} + \frac{1}{k_2^2} \leq \frac{1}{2}$, so that inflation can be realized even when the individual potentials are not too steep. It turns out that when we have an aether field and a scalar field, we can also get 'assisted inflation' as long as $a_2 \leq \frac{2}{\sqrt{3}}$. We could no longer have any periodic orbits in the interior of the state space as well as the presence of the cosmological constant in the neww set of variables explored in Case III. However, they would still occur on the boundary and since the other eigenvalue is negative, these are called asymptotic periodic orbits. Having said that, we also can attain a new sink where the scalar field, cosmological constant and aether field can all be present at late times.

As in many other models, we are trying to analyze the evolution of the universe on cosmological timescales with the matter in the universe being modelled as a scalar field with an exponential potential and a cosmological constant. We can also do this analysis in the context of different geometries and in this case, the Kantwoski-Sachs metric describes the geometry that fits our assumptions about the universe we are trying to describe. The study of cosmology often starts with some underlying, fundamental assumptions about the universe from observation. So it is important to underscore the fact that in this case we are trying to challenge the assumption that the universe is truely isotropic, based on the CMB data that we discussed in the introductory section of this paper. So if we relax the assumption that things are truely isotropic we introduce a shear term within the Kantowski-Sachs framework and our model can develop some more interesting behaviour compared to the basic scalar field cosmology of Case I. There are other attributes of a perfect fluid such as viscosity that have not been considered, but only by relaxing our assumption of isotropy were we able to include the shear term.

Pure quintessence and modified quintessence (referring to purely exponential or modified exponential potentials) models have been studied because of their simplicity and effectiveness in describing our observations [3]. The models with modified exponential potentials have shown evidence of the possiblity of a universe undergoing accelerated expansion different from ΛCDM [3]. It has also been shown that Kantowski-Sachs models with simple exponential potentials can 'isotropize' the perfect fluid at late times [3], in which the period of accelerated expansion is said to be the cause of the isotropization of both the fluid and the expansion anisotropy.

Essentially, if we observe near flat and isotropic accelerated expansion at the current time does not forbid dark energy with an anisotropic equation of state. Although Case Ia and Case Ib are relatively simple models that seem to have dynamics that model our observed reality, it turns out that the parameter values which make this model possible are too small from what have been observed [3]. As we mentioned in the introduction, Kantowski-Sachs models have become increasingly popular since a better analysis of the CMB data has led to the conclusion that we cannot statistically discard the variations in the background temperature and for that reason, the Kantowski-Sachs metric reflects a fundamental assumption of anisotropy.

As in [27], in the last two cases we studied closed Kantowski-Sachs models and the early time attractors were Kasner-like (C^+) - a circle of equilibria in the phase space. When the Vacuum Kantowski-Sachs (KS_δ) equilibrium points exist in the physical phase space, i.e. when $c < \frac{1}{2}$ we have that KS_+ is a source and KS_- is a sink. Additionally, there are a few more points which are late time attractors. First, for the Kasner-like points, if $k^2 > \frac{3}{2}$ and $\Phi > \sqrt{\frac{3}{2}}k$ the these points are sinks. For the isotropic points (FR^+_δ), if $\Psi < \frac{1}{\sqrt{6}k}$ then this is a zero curvature, non-inflationary sink. Lastly, the Bianchi Type I points (BI^+_δ) are non-inflationary periodic orbits. BI^+_- is always an unstable center. BI^+_+ is unstable if $K + (4kc)^2 > 0$ and is a stable center if $K + (4kc)^2 < 0$. The stability of the points we mentioned is for the $Q = 1$ invariant set. For the $Q = -1$ invariant set, the eigenvalues have the opposite sign as in $Q = 1$ and the coordinates are as shown in [27]. In the final case, we found four new points in the lower dimensional invariant set $x \neq 0$. As in Case I, we needed to use a non-linear method to analyze some of these equilibria in Case III. We found that there are two sinks and two sources in the $x \neq 0$ invariant set. Point a) has the cosmological constant and expansion scalar of the aether being important at late time. All of these points in the new invariant set $x \neq 0$ are non-inflationary. That means that the point e) is a late time attractor where the scalar field, aether field and cosmological constant are non-negligible at late times and depend on the interaction of the aether field and scalar field via the coupling term, a_2.

Bibliography

[1] Y Akrami, F Arroja, M Ashdown, J Aumont, C Baccigalupi, M Ballardini, AJ Banday, RB Barreiro, N Bartolo, S Basak, et al. Planck 2018 results. i. overview and the cosmological legacy of planck. *arXiv preprint arXiv:1807.06205*, 2018.

[2] B Alhulaimi, RJ Van Den Hoogen, and AA Coley. Spatially homogeneous einstein-aether cosmological models: scalar fields with a generalized harmonic potential. *Journal of Cosmology and Astroparticle Physics*, 2017(12):045, 2017.

[3] HY Chang and RJ. Scherrer. Reviving quintessence with an exponential potential. *arXiv: Cosmology and Nongalactic Astrophysics*, 2016.

[4] AA Coley and RJ Van Den Hoogen. Dynamics of multi-scalar-field cosmological models and assisted inflation. *Physical Review D*, 62(2):023517, 2000.

[5] E Corbelli and P Salucci. The extended rotation curve and the dark matter halo of m33. *Monthly Notices of the Royal Astronomical Society*, 311(2):441–447, 2000.

[6] Pea de Bernardis, P AR Ade, JJ Bock, JR Bond, J Borrill, A Boscaleri, K Coble, BP Crill, G De Gasperis, PC Farese, et al. A flat universe from high-resolution maps of the cosmic microwave background radiation. *Nature*, 404(6781):955–959, 2000.

[7] R Descartes. *Le Monde: Ou Traité de la Lumière*, volume 2. Abaris Books, 1979.

[8] W Donnelly and T Jacobson. Coupling the inflaton to an expanding aether. *Physical Review D*, 82(6):064032, 2010.

[9] G Efstathiou, JR Bond, and SDM White. COBE background radiation anisotropies and large-scale structure in the universe. *Monthly Notices of the Royal Astronomical Society*, 258(1):1P–6P, 1992.

[10] A Einstein. Zur elektrodynamik bewegter körper. *Annalen der physik*, 322(10):891–921, 1905.

[11] PM Garnavich, RP Kirshner, P Challis, J Tonry, RL Gilliland, RC Smith, A Clocchiatti, A Diercks, AV Filippenko, M Hamuy, et al. Constraints on cosmological models from hubble space telescope observations of high-z supernovae. *The Astrophysical Journal Letters*, 493(2):L53, 1998.

[12] M Gasperini. Singularity prevention and broken lorentz symmetry. *Classical and Quantum Gravity*, 4(2):485, 1987.

[13] AH Guth and PJ Steinhardt. The inflationary universe. *Scientific American*, 250(5):116–129, 1984.

[14] S Herrmann, A Senger, K Möhle, M Nagel, EV Kovalchuk, and A Peters. Rotating optical cavity experiment testing lorentz invariance at the 10- 17 level. *Physical Review D*, 80(10):105011, 2009.

[15] WM Hicks. The michelson-morley experiment. *Philos. Mag. S*, 6(3):256, 1902.

[16] M Janssen and J Stachel. The optics and electrodynamics of moving bodies. 2004.

[17] E Kasner. Geometrical theorems on einstein's cosmological equations. *American Journal of Mathematics*, 43(4):217–221, 1921.

[18] A Liddle. *An introduction to modern cosmology*. John Wiley & Sons, 2015.

[19] AP Lightman. *Ancient light: our changing view of the universe*. Harvard University Press, 1993.

[20] A Patrik, AA Coley, G Leon, and SJ Latta. Spherically symmetric einstein-aether perfect fluid models. *arXiv preprint arXiv:1508.00276*, 2015.

[21] P James E Peebles and B Ratra. The cosmological constant and dark energy. *Reviews of modern physics*, 75(2):559, 2003.

[22] S Perlmutter, B P Schmidt, and AG Riess. The nobel prize in physics 2011. *AG Riess, My Path to the Accelerating Universe, Nobel Lecture*, 2011.

[23] AI Sabra et al. *The optics of Ibn al-Haytham: Books I-III: On direct vision*, volume 1. Warburg Institute, University of London, 1989.

[24] A Sandage. Edwin hubble 1889-1953. *Journal of the Royal Astronomical Society of Canada*, 83:351, 1989.

[25] G F Smoot, CL Bennett, A Kogut, EL Wright, J Aymon, NW Boggess, ES Cheng, G De Amici, S Gulkis, MG Hauser, et al. Structure in the cobe differential microwave radiometer first-year maps. *The Astrophysical Journal*, 396:L1–L5, 1992.

[26] DN Spergel, L Verde, H V Peiris, E Komatsu, MR Nolta, CL Bennett, M Halpern, G Hinshaw, N Jarosik, A Kogut, et al. First-year wilkinson microwave anisotropy probe (wmap) observations: determination of cosmological parameters. *The Astrophysical Journal Supplement Series*, 148(1):175, 2003.

[27] RJ Van Den Hoogen, AA Coley, B Alhulaimi, S Mohandas, E Knighton, and S O'Neil. Kantowski-sachs einstein-aether scalar field cosmological models. *Journal of Cosmology and Astroparticle Physics*, 2018(11):017, 2018.

[28] S Wiggins. *Introduction to applied nonlinear dynamical systems and chaos*, volume 2. Springer Science & Business Media, 2003.

[29] MF Wondrak. The cosmological constant and its problems: A review of gravitational aether. In *Experimental Search for Quantum Gravity*, pages 109–120. Springer, 2018.